

RESEARCH OUTPUTS / RÉSULTATS DE RECHERCHE

Numidian clay deposits as raw material for ceramics tile manufacturing

Moussi, B.; Hajjaji, W.; Hachani, M.; Hatira, N.; Labrincha, J. A.; Yans, J.; Jamoussi, F.

Published in:
Journal of African Earth Sciences

DOI:
[10.1016/j.jafrearsci.2020.103775](https://doi.org/10.1016/j.jafrearsci.2020.103775)

Publication date:
2020

Document Version
Peer reviewed version

[Link to publication](#)

Citation for pulished version (HARVARD):
Moussi, B, Hajjaji, W, Hachani, M, Hatira, N, Labrincha, JA, Yans, J & Jamoussi, F 2020, 'Numidian clay deposits as raw material for ceramics tile manufacturing', *Journal of African Earth Sciences*, vol. 164, 103775. <https://doi.org/10.1016/j.jafrearsci.2020.103775>

General rights

Copyright and moral rights for the publications made accessible in the public portal are retained by the authors and/or other copyright owners and it is a condition of accessing publications that users recognise and abide by the legal requirements associated with these rights.

- Users may download and print one copy of any publication from the public portal for the purpose of private study or research.
- You may not further distribute the material or use it for any profit-making activity or commercial gain
- You may freely distribute the URL identifying the publication in the public portal ?

Take down policy

If you believe that this document breaches copyright please contact us providing details, and we will remove access to the work immediately and investigate your claim.

Manuscript Number: AES7683R1

Title: Numidian clay deposits as raw material for ceramics tile manufacturing

Article Type: Research Paper

Keywords: Keywords: Clays, Tabarka, Sejnane; Ceramic tiles; Technological parameters, Tunisia.

Corresponding Author: Professor Bechir Moussi, PhD

Corresponding Author's Institution: Water Researches and Technologies Center

First Author: Bechir Moussi, PhD

Order of Authors: Bechir Moussi, PhD; Walid Hajjaji; Mondher Hachani; Nouri Hatira; Joao António Labrincha; Johan Yans; Fakher Jamoussi

Abstract: We investigate the potential use in traditional ceramics of several clays collected in the Numidian Flysch Formation (Upper Oligocene) at Tabarka, and Sejnane; Northern part of Tunisia). The valorization of these adopts the technique of dry process, which requires a mixture of powdered clay with 7% water. This allows rapid drying of uncooked tiles. The tiles are fired at four different temperatures (1000°C, 1050°C, 1100°C and 1150°C) in order to optimize technological parameters such as shrinkage, water absorption and flexural strength. The obtained tiles show acceptable drying and firing shrinkage (not exceeding 3%), and bending strength (between 13 and 16 N/mm²) which are close to the required standards (EN ISO 10545-4, 15N/mm² for wall tiles). The absorption ranges from 10 to 20%, which classifies these products in group BIII according to the international standards (ISO 13006 and EN ISO 10545-3). Variation of shrinkage and water absorption with the firing temperature reveals that optimal range is 1125-1150°C for the Tabarka samples, whereas the Sejnane products might be fired at lower values (~1025°C). The Tabarka fired pieces exhibit strong brightness. These results suggest that these latter clays could be used for white products such as sanitary ware formulations while those from Sejnane ones are more appropriated for colored (red) applications. The X-ray diffraction on the fired tiles powders shows the formation of quartz which is initially present in the crude clays, and mullite that is present at all firing temperatures. Moreover, the presence of mullite due to the richness of Al₂O₃ in Tabarka clays could support their refractory properties.

Research Data Related to this Submission

There are no linked research data sets for this submission. The following reason is given:

No data was used for the research described in the article

SUBMISSION OF PAPER

Dear editor,

We are attaching the paper entitled " **Numidian clay deposits as raw material for ceramics tile manufacturing**" submitted to **Journal of African Earth Science**. The authors are:

B. Moussi, W. Hajjaji, M. Hachani, N.Hatira, J.A. Labrincha, J. Yans' F.Jamoussi

The complete address of the corresponding author is:

Bechir Moussi, PhD

Water Research and Technologies Centre Borj Cedria

Goressources laboratory

273 CERTE, Soliman, Tunisia 8020

Fax: +216 79 325 802

Email: bechirmoussi2007@gmail.com

: bechir.moussi@issatgb.rnu.tn

Sincerely yours,

B. Moussi

1/10/2020

Reviewer #1:

Main comments:

Authors refer along the text to "clay samples", but it is better to write "clayey samples".

Corrected

The granulometry is coarser than in a common clay (>60% are greater than 2 microns), and the quartz content is very high.

The particle size distribution was carried out by the series of sieves on the clays and the sand and then supplemented by the laser microgranulometry on the clayey fraction lower than 63 micrometers.

With the observed value of Fe_2O_3 content, sample O1 can have a maximum of 11% of siderite, and not 18%;

with the observed value of CaO content, sample RGS can have a maximum of 14% of calcite, and not 22%;

with the observed value of K_2O , sample O1 cannot have 20% of illite and 7% of I-S, and only a maximum of 2% illite is compatible with 0.16% of K_2O in this sample.

Calculation of percentages of minerals was rectified using XRD and chemical analysis. New values are then given.

Sample RGS. Please describe this sample in the "Methods" section, and the reason to select it for mixtures. A similar comment can be done for "Sand" and "Feldspar" samples.

Completed and I give the reason for use

Problems in figure numbers. From figure 2, they are wrong. Please carefully revise them and place right numbers to figures along the text.

Corrected

Line 183. Sample O1 do not show higher illite content. Please revise and try to find other arguments.

The Holtz & Kovacs (Fig. 3) classified these clays as moderate plastic, with the exception of O4 which is considered highly plastic. The large amount of clay minerals (75%) can explain this plasticity behavior of this last sample.

In fact I made a mistake, it is the sample O4 and not O1 has a highly plastic behavior

Line 187. Sample O1 includes only 0.16% of K_2O . For this reason, this sentence is not true. Perhaps something is wrong with the chemical analysis.

The calculation of the percentage of the minerals has been rectified based on the chemical analyzes therefore the amount of illite is reduced and what makes the phrase right.

Line 192. The Tabarka clays do not show higher phyllosilicates content. Please rewrite the sentence.

Nevertheless, the Tabarka clays are relatively finer (Fig.4) this is probably due to the fineness of the quartz particles and the phyllosilicates richness (~ 65%).

Lines 207-209. Samples exhibited similar phyllosilicate content. So, this is not the reason. Besides, sample O4 do not include mixed-layers I-S.

A higher shrinkage is recorded on the Sejnane samples due to the richness in melting (sum Fe_2O_3 , MgO , CaO , Na_2O and K_2O equal to 11%) compared to Tabarka clays (4%). These fluxes tend to promote vitrification and increase shrinkage (Tite et Maniatis, 1975, in Cultrone et al., 2001)

Please revise figure legends, and indicate on it the names of the samples. Figure 6 are not "Bigot curves of the clays samples", but only of two of them.

Corrected

Data included on Figure 9 and table 3 are the same. No need to include both, figure and table, on the manuscript. Please select only one of them. Besides, lines 216-217 repeat the same data. Please delete it.

I deleted figure 8. The table must remain in the manuscript; lines 216-217 are deleted

Along the text there is confusion with the names of the samples. Sometimes Tabarka is used, and others Sidi Bader, or Sidi El Bader, and sometimes Sejnane and others Om Tebal. Please homogenize the names when referring to samples. In any case, I do not know the reason to call samples S8, S9, O1 and O4. It is better to use S1, S2, O1 and O2.

The names of samples in the text were modified (Tabarka and Sajnane)

The samples were named according to their location in the lithological log. If I change S1, S2, T1 and T2, there will then be an incompatibility with the lithological section.

I am not sure that figures including x-ray diffractograms are necessary.

Figure including x-ray diffractograms are deleted

Minor comments:

Line 74. The verb "is" is lacking. Besides, "papers" must be "paper"

"is" added

Line 86. To delete the parenthesis before "acronym". If not, when cited Guerrero et al., 1993, there will be two of them.

Parenthesis deleted

Line 95. ...to fill high density...? Something is lacking here.

Sediment density = significant thickness of sediment

The sediments were deposited in a large complex of turbidite channels to fill high sediment density observed over tens of kilometers

Line 112. Talbi, 1998 (not Talbi et al.,)

Rectify

Line 134. Write greeks letters for alpha and lambda.

(Cu-K α radiation (1,540598Å),

Line 149. alfa alumina? Please revise and write greeks letter.

By using α -Al₂O₃

Line 179. were also (not "was also)

Corrected remark

Lines 201-204. To delete. I do not know why authors include this sentence here. It adds nothing.

Deleted

Line 219. ...BIII group of international standards. Please add reference here

BIII group of international standards (ISO 13006)

Lines 221-222. This must be described in the "Method" section.

This part was added in method section

Line 225. A good pressure? Please indicate the value for this.

A good pressure (280-250 bars)

Lines 232-233. Figure 10 correlates Firing temperature and Firing shrinkage. Please revise.

The numbers of the figures and their attributions have been revised.

Lines 250-251. Microstructure is not detected by X-ray diffractometry. Please rewrite

The fired ceramics tiles MS8 show a mineralogical composition formed by mullite, quartz, and diopside, detected by X-ray diffraction (Fig. 9).

Figure 12. Legends for minerals in the diffraction peaks are very close among them. It is very difficult to read.

Corrected

Figure 13. Please indicate on the microphotos the name of the samples, and the temperature (line252).

Corrected

Line 259. Addition of carbonated clay... Authors add 20% of RGB to all the mixtures. Please explain the reason to maintain this percentage in all cases.

The addition of carbonated clay reduced the firing temperatures. Carbonated clay (RGS) was added (20%) in all mixtures with the aim of increasing the CaO content and promoting the formation of a glassy phase (Kazmi et al., 2017) because these crude clays have a low CaO content (table 1). Moreover, the presence of calcite, dolomite or both can influence the formation of different minerals at high temperatures (Trindade et al., 2010). The presence of fluxing oxides including Fe_2O_3 tend to reduce the temperature at which a partial melt is formed (Abdelmalek et al., 2017). The iron oxide is the main colorant in clayey materials, responsible for the reddish color observed after firing (Abajo, 2000).

Line 641. Figure 67?

Corrected

Reference Holtz & Kovacs (1981) is not included s not included in the reference list

Reference added

Homogenize references. Sometimes the year of publication is not among brackets
Please add Tunisia in keywords

References have been revised

Reviewer #2:

Title changed

Numidian clay deposits as raw material for ceramics tile manufacturing

INTRODUCTION: the state of the art about the use of Numidian clays, particularly those from Tabarka and Sejnane, is missing. In particular, I cannot see any reason why the previous study: Bennour, A., Mahmoudi, S., Srasra, E., Boussen, S., & Htira, N. (2015). Composition, firing behavior and ceramic properties of the Sejnène clays (Northwest Tunisia). *Applied Clay Science*, 115, 30-38, has been neglected. Please, define better the current level of knowledge on ceramic uses of Numidian clays (not only in Tunisia, if possible) and consequently improve the aims of the manuscript.

Rectified introduction

In this perspective, and for the purpose of researching clay deposits for ceramics, several research studies on Tunisian clay materials have been carried out (Baccour et al., (2009); Khemakhem et al., (2009). Hajjaji et al., (2010). Medhioub et al., (2010). Hachani et al., (2012). Hedfi et al., (2014, 2016); Ben M'barek Jemai et al., (2015); Hammami-Ben Zaied et al., (2015); Bennour et al., (2015, 2017); Ben Salah et al., (2016, 2018); Boussen et al., (2016); Mahmoudi et al., (2016, 2017); Zouaoui et al., (2017); Chihi et al., (2019); Kamoun et al., (2019)).

The aim of this article is to use the Numidian clays from the Tabarka and Sejnane region, which are developing regions in the ceramic industry, compare the products obtained and provide a database that could be used by investors.

Numidian clays from Sejnane have been studied and valorised in the field of ceramics (Bennour et al., 2015; Moussi, 2012). Bennour et al. (2015) studied the composition and firing behavior of these clays as a material for ceramics. Moussi (2012) studied the suitability of the Numidian clays of Cap Serrat, Gamgoum, Om Tebal and Aouinet to be used in ceramic tiles. He proved that these clays can provide important potential raw material for the manufacture of ceramic tiles. Industrially these clays are very little used in the manufacture of ceramic tiles because of their distance from the factories which are dense in the Tunisian coastal region and Cap Bon. Some small deposits are exploited for artisanal pottery.

MATERIALS: one sample, RGS, was not described.

The description of RGS was done

METHODS: standard deviation must be indicated in all tables and error bars in graphs.

Added on table N1 and 3, error bar added on fig. 8

About Bigot curves, better to indicate the criterion followed to choose the water amount).

The shaping of the clay into pieces of dimension 15x15x30mm (to measure the weight and length of wet pieces) requires adding water to the raw powder until a normal paste that does not stick to fingers is acquired (until 25-30%).

RESULTS should be compared with the literature about ceramic clays in Tunisia (and other countries, if possible) in terms of chemical and mineralogical composition and particle size distribution. Otherwise, the manuscript appears to be a mere technical report.

A comparison has been made

RESULTS, XRD: it should be better, since samples are just four, to show all patterns (at least as supplementary material). In fact, it is not possible to compare sample O1, which is said to contain I/S mixed-layers, with S9 that appears in Fig. 3, that apparently contains some mixed-layers as well.

The first Reviewer asked to remove the X-ray diffractograms, he assumed it was useless to show them. otherwise i have all drx and i can add them

RESULTS, XRF: all sums close far from 100%; this is despite loss on ignition is higher than expectable from mineralogical composition; any explanation? It is not related which is the source of some components: MgO (especially in samples O), Na₂O in O1, Fe₂O₃ in all samples but O1, CaO in all samples but RGS. This will be important during discussion about firing transformations!

The total loss on ignition is relatively high in the Tabarka samples (10.78%) compared to the Sejnane samples (9.77%). This loss on ignition is dependent on the decomposition of clay minerals (kaolinite), the removal of absorbed and crystalline water and the alkali content. The high loss on ignition detected in RGS carbonate clay is 14.35%, it is due to the decomposition of kaolinite and carbonates.

RESULTS, XRD vs XRF: data unfortunately do not always match! O1: quartz seems to be in defect for available silica; illite and siderite are in excess with respect to available K₂O and Fe oxide, respectively; perhaps, a (Fe,Mg)CO₃ term? and a Na-rich I/S instead of illite? S8 and S9: similar chemical composition but strongly different % of kaolinite and illite; quartz % seems to be in excess.

Calculation of percentages of minerals was rectified using XRD and chemical analysis. New values are then given.

TABLE 1: decimal separator must be point. TABLE 2: % wt missing.

Done

RESULTS, PARTICLE SIZE should be discussed more in detail, as from Fig. 5 there are peculiar distributions, like O clays: sand+clay fractions and practically no silt!

The discussion on particle size curves is detailed

RESULTS, PLASTICITY should be discussed with reference to both particle size and mineralogy, particularly the occurrence of expandable clay minerals.

The discussion on plasticity is changed.

The Holtz & Kovacs (Fig. 3) classified these clays as moderate plastic, with the exception of O4 which is considered highly plastic. The large amount of clay minerals (75%) can explain this plasticity behavior of this last sample. Hajjaji et al. (2010) have shown that when the quantity of phyllosilicates increases, the limits of Atterberg also increase. This plastic behavior of the samples is closely related to the presence of coarse grains of silts and sands as well as the mineralogical composition. Although these clays are placed above the domain of kaolinite and illite in the diagram of Holtz & Kovacs these clays are rich in kaolinite this is explained by the richness in grain of sand which decrease the index of plasticity.

RESULTS, BIGOT CURVE: which is a suitable behavior for industrial clays in Tunisia (or elsewhere?)

Result Bigot curves was rectified

The drying behavior is a parameter used in the ceramic industry as the prime indicator for selection of the raw material (Dondi et al., 1998, Meseguer, 2010). This behavior is deduced from the Bigot curves. According to the curves, we notice a total mass loss of 20.8% for the Tabarka clays and 25.5% for the Sejnane clays. This loss of mass is characterized by two stages. The first mass loss consists of the colloidal water loss which is 14.61% for the Tabarka clays and 10.07% for that of Sejnane. This proves that the latter are characterized by a faster drying than Tabarka clays. The second loss of mass is linked to the departure of the interposition water which are 6.19% and 15.45% respectively for S9 and O1. According to these results, Tabarka clays have a slow drying behavior which suggests the addition of a degreaser.

RESULTS, MINERALOGY OF FIRED bodies: gehlenite is cited at line 202, but diopside appears in Figs 11-12, which of the two?

Gehlenite is a transient phase which does not appear in favor of the diopside. these lines 201-204 have been deleted.

Albite-anorthite-sanidine are reported at line 246, but from XRD patterns it can hardly concluded about the occurrence of three different feldspars, newly formed during firing

According to the XRD results, albite and anorthite are present but sanidine does not appear. But according to Lee et al. (2003) these three phases appear together. in this case it is necessary to delete the the sanidine formation.

"as well as potassic feldspars (sanidine)" this term was deleted

! Even the occurrence of mullite, looking in detail at XRD patterns is questionable. Suggestion: put an inset in Figs 11 and 12 with enlarged pattern, e.g. 20-40°2theta or so, to support your interpretation.

The discussion of the XRD models for the fired product is rewritten to show the formation of mullite and the other phases.

Since some figures have been deleted, the numbers of figures 11 and 12 become 9 and 10.

Figures 9 and 10 of XRD are revised.

The firing transformations are represented by X-ray diffraction in figures 9 and 10. The X-ray diffractions of the raw mixtures before firing are compared with those fired at 1000, 1050, 1100 and 1150 °C. The crude mixtures show the richness in Kaolinite and in illite in the presence of quartz. According to DTA, the kaolinite disappears at 550°C, on the other hand from 1000°C (both case of MO1 1000 and S8 1000) the amount of illite decreases to disappear at 1050 ° C. From 1100 ° C, the beginning of the formation of mullite is recorded (reference code: 2-431) marked by the peak at 5.39Å. Mullite is an important ceramic material because of its low density, high thermal stability, and stability in severe chemical environments (Cao et al., 2004). For a higher temperature (1150 °C), a peak at 4.06Å only for fired products of Tabarka records the formation of cristobalite (reference code 1-76-939). A peak at 2.94Å appears on the X-rays diiffractograms of the all fired product of Tabarka and Sejnane attributed to the formation of the diopside (reference code 1- 83-1820). The Sejnane clays are rich in iron oxide (Table 1). These iron oxides contributed to the formation of hematite (Fig.10) recorded only on fired products of Sejnane and marqué by a peak at 2.69Å (code reference 1-1053) which ensures a certain rigidity of the ceramics tiles (high bending strength), due to its fluxing character. The quartz initially present in the mixtures of raw clays persists during all firing phases. The presence of silicon, alkaline and calco-alkali compounds support the formation of plagioclases (albite and anorthite) (Lee et al., 2008) which appear from 1000 ° C but their quantities increase depending on the temperature.

RESULTS, TECHNOLOGICAL DATA are compared with standard requirements for wall tiles that are usually attained by the ceramic industry using carbonate-containing clays (there are clear guidelines in the literature). Mention should be done that batches were designed to maximize the use of Numidian clays and improvements are expected by properly adjusting the recipes.

TECHNOLOGICAL DATA

In this work, we tried to popularize the quality of these Numidian clays to businessmen to invest in the northwest of Tunisia. These clays are devoid of carbonates. However, the amount of RGS carbonated clay added which contains 14% calcite is 20% in the mixtures. This means that the amount of calcite in the mixture does not exceed 3% (2.8%). The purpose of adding this clay is to create more fluxing to promote the densification and vitrification of the products, and to improve the resistance to bending.

CONCLUSIONS: I would have expected some general statement about geology > mineralogical composition > properties > possible uses (you have submitted to the J Afr Earth Sciences, not a ceramic journal!).

Conclusions modification

The Tabarka and Sejnane clays, which belong to the Numidian Flysch, whose thicknesses can reach 3000 meters, were studied in order to decipher their use in ceramic manufacturing. The characterization of the raw clays shows a mineralogy composition dominated by kaolinite and illite and relatively high quartz content for the two sites of Tabarka and Sejnane. Chemical analyzes show a significant richness in SiO_2 ; this can be explained by the presence of clays and silica sand. The mineralogical and chemical results are consistent. According to the particle size distribution curves, the Sejnane clays have a larger coarse particle size fraction compared to those of Tabarka which influences the percentage of sand additions as degreaser. These clays were tested in the manufacture of ceramic tiles. Technological tests show the aptitude of these raw materials to be used in the manufacture of ceramic tiles on an industrial scale. The aspect of ceramic tiles is acceptable with characteristics close to the required standards. In particular, the drying and firing shrinkages are low, the flexural strength and the water absorption are also within the standard limits. Tabarka ceramic tiles have a white color due to the richness in kaolinite and the rarity of iron oxides. These clays can be used as raw materials for ceramic tiles. Sejnane ceramic tiles have a red color due to the richness of iron oxide initially present in raw clays. These very abundant Numidian clays alternate in succession with metric, sometimes decametric, levels of consolidated sandstone. These geological outcrops extended to the northwest of Tunisia in the Tellian domain, present immense geological deposits of industrially useful raw material.

1
2
3
4 **Highlights**
5

6
7 Potential use in traditional ceramics of Numidian Flysch was investigated
8

9 Obtained tiles show acceptable firing shrinkage 3% and bending strength at 16 N/mm²
10

11 Shrinkage and WA optimal range is 1150°C for Tabarka and 1025°C for Sejnane samples
12

13
14 Fired tiles shows the formation mullite, especially in Tabarka clays richer in Al₂O₃
15

16 Abundant clayey geological raw material of Numidian can be used on ceramic industry
17
18
19
20
21
22
23
24
25
26
27
28
29
30
31
32
33
34
35
36
37
38
39
40
41
42
43
44
45
46
47
48
49
50
51
52
53
54
55
56
57
58
59
60
61
62
63
64
65

Numidian clay deposits as raw material for ceramics tile manufacturing

B. Moussi^{1*}, W. Hajjaji², M. Hachani³, N. Hatira⁴, J.A. Labrincha⁵, J. Yans⁶ & F.

Jamoussi¹

1 Georessources Laboratory, CERTE, 273 - 8020 Soliman, Tunisia

2 Natural Water Treatment Laboratory, CERTE, 273 - 8020 Soliman, Tunisia

*3 University of Carthage Higher Institute of Environmental Science and Technology of
Borj Cedria, B.P. n° 1003 2050 Hammam Lif, Tunisia*

*4 National Office of Mines 24, Street of Energy, 2035 - Charguia – Tunis, BP: 215-
10801 Tunis Cedex – Tunisia*

*5 Materials and Ceramic Engineering Dept & CICECO. University of Aveiro. 3810-193
Aveiro. Portugal*

*6 Department of Geology, University of Namur, ILEE, Institute of Life, Earth and
Environment - 61, rue de Bruxelles, B-5000 Namur, Belgium*

* Author to whom correspondence should be addressed; phone: +216 58 795 598; fax: +216

79 325 802; email: bechirmoussi2007@gmail.com

Abstract

We investigate the potential use in traditional ceramics of several clays collected in the Numidian Flysch Formation (Upper Oligocene) at Tabarka, and Sejnane; Northern part of Tunisia). The valorization of these adopts the technique of dry process, which requires a mixture of powdered clay with 7% water. This allows rapid drying of uncooked tiles. The tiles are fired at four different temperatures (1000°C, 1050°C, 1100°C and 1150°C) in order to optimize technological parameters such as shrinkage, water absorption and flexural strength. The obtained tiles show acceptable drying and firing shrinkage (not exceeding 3%), and bending strength (between 13 and 16 N/mm²) which are close to the required standards (EN ISO 10545-4, 15N/mm² for wall tiles). The absorption ranges from 10 to 20%, which classifies these products in group BIII according to the international standards (ISO 13006 and EN ISO 10545-3). Variation of shrinkage and water absorption with the firing temperature reveals that optimal range is 1125-1150°C for the Tabarka samples, whereas the Sejnane products might be fired at lower values (~ 1025°C). The Tabarka fired pieces exhibit strong brightness. These results suggest that these latter clays could be used for white products such as sanitary ware formulations while those from Sejnane ones are more appropriated for colored (red) applications. The X-ray diffraction on the fired tiles powders shows the formation of quartz which is initially present in the crude clays, and mullite that is present at all firing temperatures. Moreover, the presence of mullite due to the richness of Al₂O₃ in Tabarka clays could support their refractory properties.

Keywords: Clays, Tabarka, Sejnane; Ceramic tiles; Technological parameters, Tunisia.

1. Introduction

The Numidian Flysch is a widespread Formation of the Tell chain located in the Northern part of Tunisia. It contains successions of clayey levels and consolidated sandstones. Previous works have been conducted to refine the geological knowledge of the Numidian Flysch (e.g., Rouvier, 1977; Fildes et al., 2009; Yaich et al., 2000; Bouaziz et al., 2002; Talbi et al., 2008; Riahi et al., 2010). Other studies have documented Pb-Zn mineralizations associated with the Numidian Clays, structurally controlled by hydrothermalism (e.g. Decree et al., 2008; Abidi et al., 2010; Jemmali et al., 2011, 2013). Felhi et al. (2008) characterized the Numidian kaolinitic clays of Tabarka.

Although Tunisia is a small country (163,610 km²), the production of ceramic tiles is developing steadily (26 million m² in 2007, growing by 12% in the last five years), due to the increasing demands of national building programs and challenges created by new opening markets (Moussi et al., 2011). There are approximately 94 Tunisian factories specialized in ceramic manufacturing, consuming about 420.000 tons in 2011 (Jeridi et al., 2014) and the development of the construction sector. Constant efforts of the economic development offices are focused on exploration for new deposits to support the increasing consumption needs, and the widespread ceramic production sites (Medhioub et al., 2012).

In this perspective, and for the purpose of researching clay deposits for ceramics, several research studies on Tunisian clay materials have been carried out (Baccour et al., (2009); Khemakhem et al., (2009). Hajjaji et al., (2010); Medhioub et al., (2010). Hachani et al., (2012); Hedfi et al., (2014, 2016); Ben M'barek Jemai et al., (2015); Hammami-Ben Zaied et al., (2015); Bennour et al., (2015, 2017); Ben Salah et al.,

(2016, 2018); Boussen et al., (2016); Mahmoudi et al., (2016, 2017); Zouaoui et al., (2017); Chihi et al., (2019); Kamoun et al., (2019)).

The aim of this article is to use the Numidian clays from the Tabarka and Sejnane region, which are developing regions in the ceramic industry, compare the products obtained and provide a database that could be used by investors.

Numidian clays from Sejnane have been studied and valorised in the field of ceramics (Bennour et al., 2015; Moussi, 2012). Bennour et al. (2015) studied the composition and firing behavior of these clays as a material for ceramics. Moussi (2012) studied the suitability of the Numidian clays of Cap Serrat, Gamgoum, Om Tebal and Aouinet to be used in ceramic tiles. He proved that these clays can provide important potential raw material for the manufacture of ceramic tiles. Industrially these clays are very little used in the manufacture of ceramic tiles because of their distance from the factories, which are dense in the Tunisian coastal region and Cap Bon. Some small deposits in the northwest of Tunisia were exploited for artisanal pottery.

2. Geological setting

Clays collected for this study belong to the Numidian Flysch Formation, Oligocene-Miocene in age (Rouvier, 1977; Felhi et al., 2008; Riahi et al., 2010). The Numidian Flysch results from the infilling of a peri-Mediterranean basin created between the two main tectonic events related to the Alpine Maghrebide belt (e.g. Guerrera et al., 1993 and references therein; Frizon de Lamotte et al., 2000). The first event was linked to the subduction of the Tethyan oceanic strip that separated Gondwana and the Alcapecac acronym from “Alboran basin” and the main internal massifs, from west to east

Kabylian massifs in Algeria, Peloritan Mountains in Sicily and Calabria (see Guerrera et al., 1993). The second is known as the Alpine phase and was formed by collision between the dismembered Alkapeca region and Africa. The West Mediterranean oceanic basin was created between these two main events, with an initial rifting stage (30-21 Ma, i.e., late Oligocene-Aquitania) followed by a drifting stage with the Sardinia's counterclockwise rotation during Burdigalian-Serravalian (Jolivet et Faccenna, 2000).

The sediments were deposited in a large complex of turbidite channels to fill high sediment density observed over tens of kilometers (Yaich et al., 2000). This series can locally reach ~3000 m thick and consists of three lithological units (Rouvier 1977, 1994). The series of Zouza is the lower unit; Late Oligocene in age, and has a thickness of ~1000 m in the Nefza region. It consists of a succession of sandstone lenses, clays locally oxidized, and quite rare conglomeratic horizons. The middle unit is Kroumirie sandstones, Late Oligocene in age. This latter is composed of layers of sandstone, clay and conglomerates with pebbles of quartz. The upper unit or series Babouch, Early Miocene in age, consists of gray clays. Based on planktonic foraminifera biozones, Yaich et al. (2000) date the Numidian Formation in an interval comprised between Early Rupelian and Early Burdigalian. Riahi et al. (2010) present a new dating (Oligocene to early Miocene) for the two first units, based on new biostratigraphic data from the analysis of planktonic foraminifera. Yaich et al. (2000), mean while, proposed the establishment of the Numidian between Langhian and Serravallian (13 Ma), corresponding to the intrusion of endogenous igneous rocks in the area (see Decrée et al., 2014).

The origin of the sediments forming the Numidian was widely debated. The provenance from the North is based on the presence of current ripples in Numidian formations (Wildi, 1983; Parize et al., 1986; Talbi, 1998). This hypothesis is consistent with recent studies that suggest a European Nordic sediment provenance, based on the study of zircons (Fildes et al., 2009). Alternatively, Wezel (1970), based on the morphology of quartz grains, proposes a Southern source of Numidian, from the Nubian Sandstone. Accordingly, the analysis of sedimentary structures by Hoyez (1975) suggests that the Numidian is located at the edge of Saharian zone. This hypothesis was recently overturned by Yaich et al. (2000), based on biostratigraphic arguments. Anyway, the origin of the kaolinitic-illitic clays would be related to the weathering/alteration of the feldspars of the Numidian Flysch (Crampon, 1973). The area experienced complex phases of weathering and alteration, leading to the neoformation of halloysite/kaolinite in several rocks (Decree et al., 2008; Sghaier et al., 2014). The lithological succession (Fig. 1 and 2) of the two studied sites provides a good estimate of the reserves of kaolinitic-illitic clays in the area.

3. Materials and methods

Two sites were studied: Sidi El Bader close to Tabarka city and Om Tebal close to Sejnane city (Fig.1). Sidi El Bader area is located east of the town of Tabarka limited by the Jebel Touila at its east side. Four representative samples (50 kg each) were collected: S8 and S9 from Tabarka, O1 and O4 from Sejnane.

Mineralogical analyses of bulk samples were carried out by X-ray diffraction (XRD), using an X-ray Panalytical X'Pert Pro diffractometer (Cu-K α radiation (1,540598Å), 2 θ range from 3° to 60°). The relative amounts of phases were estimated by measuring the

areas of the main peaks (Torres- Ruiz et al., 1994; López-Galindo et al., 1996) using the Panalytical X'Pert HighScore Plus software. Oriented aggregates were treated with ethylene glycol and heated at 550°C for 2 h. The chemical composition of powdered samples was determined by X-ray fluorescence; with a Panalytical Axios Dispersive XRF Spectrometer using the conventional techniques (Meseguer et al., 2009). The loss-on-ignition was evaluated from the weight difference between samples heated at 100°C and 1000°C. The results are expressed in concentration percent of oxides. The Casagrande method was selected for the determination of the Atterberg limits (LCPC, 1987; Grabowska-Olszewska, 2003) with an experimental error of $\pm 3\%$. The grain-size distribution of as-received samples was obtained by wet sieving, using an AFNOR series device adopted by the French standardization system. The fraction $< 63 \mu\text{m}$ was completed by laser diffraction using Mastersizer 2000 granulometer. Thermal analyses TDA-TGA were performed using Netzsch STA409/429 equipment with a heating rate of 10 K min^{-1} and by using $\alpha\text{-Al}_2\text{O}_3$ as the inert marker. Dilatometric analysis was conducted on a Netzsch 402E dilatometer at a maximum temperature of 1000°C (5°C min^{-1} heating rate). The thermal behavior was studied by DTA-TG analyses (Setaram apparatus) in air atmosphere with $10^\circ\text{C min}^{-1}$ heating rate. The Bigot curves were obtained under room-temperature conditions by using an Adamel barelattograph. The clayey material was crushed and rolled for a coarse grain size of 1mm. The shaping of the clay requires certain amount of water into pieces of dimension 15x15x30mm (to measure the weight and length of wet pieces). These pieces were subjected to drying in open air conditions in the apparatus of Adamel Barellatograph. This device can track and trace drying curve according to the mass loss. At the end of drying, the pieces were weighed and oven dried for 24 hours at 110°C for measuring the final mass and dry

lengths. These parameters allow at measuring the drying shrinkage and water required for shaping, interposition and colloidal.

The ceramics tiles were shaped by dry pressing and the material was dried and crushed before sieving. The moisture level was adjusted to 6-7 wt% and the powders were pressed (250 bars) into 50x50x100 mm pieces (Moussi et al., 2011). These tiles were dried overnight at 40°C + 8h at 110°C. Then the samples were fired at maximum temperatures of 1000, 1050, 1100 and 1150°C (15°C/min, heating rate and 30 min dwell time), approaching industrial conditions (Jeridi et al., 2008). Shrinkage on drying and firing was determined manually. The bending strength of the fired bodies was determined on a LCV F006 NANETTI Fleximeter and the water absorption was assessed following European standards (UNI EN ISO 10545-3). Phases formed after firing were characterized by XRD while the microstructure was studied by scanning electron microscopy (SEM, Hitachi SU70, Bruker AXS detector, Quantax software). To improve the quality of ceramic products obtained with crude clays, separate mixtures were prepared by combining Tabarka and Sejnane clays with silica sand, carbonated clay (RGS) and feldspars (Table 2). These mixtures have undergone the same processes as shaping, drying and firing as previously described with ceramic tiles without additions.

Carbonated clay was added to the mixtures due to the richness of calcium carbonate (14%). An addition of carbonate is therefore desired in order to create a porosity. In fact, these carbonates are considered to be fluxes, extending glassy phases (Kazmi et al., 2017). Feldspars have been added for the same reason as a fluxing agent. Silica sand has been added to enhance the hardening qualities and increase the flexural strength.

RGS carbonate clay is collected in the Nefza region, between Tabarka and Sejnane. It is a clay of Lutetian-Bartonian age locally qualified "argile noire à boules Jaune" with dolomitic concretions. These clays belong to the tellian facies (Rouvier, 1977). The added sand belongs to the Beglia formation of lower Miocene age harvested from the Saouaf region.

4. Results and discussion

The X- ray diffraction patterns (Table 1) show a kaolinitic-illitic content of the samples collected from both studied sites. Mixed-layers I-S were also identified in O1 sample. Moreover, an important quartz fraction (superior to 25%) is detected and directly influences the rheological behavior of clays. The Holtz & Kovacs (Fig. 3) classified these clays as moderate plastic, with the exception of O4 which is considered highly plastic. The large amount of clay minerals (75%) can explain this plasticity behavior of this last sample. Hajjaji et al. (2010) have shown that when the quantity of phyllosilicates increases, the limits of Atterberg also increase. This plastic behavior of the samples is closely related to the presence of coarse grains of silts and sands as well as the mineralogical composition. Although these clays are placed above the domain of kaolinite and illite in the diagram of Holtz & Kovacs these clays are rich in kaolinite this is explained by the richness in grain of sand which decrease the index of plasticity.

This variation could lead to the appearance of cracks after drying process (Jordan et al., 1999). These results are comparable to the mineralogical study by Bennour et al., (2015). they prove the existence of kaolinite, illite and I/S mixed-layers associated with quartz. As for the study by Hammami-Ben Zaied et al., (2015), these authors studied Miocene Gram clays. They proved an excessive richness of these clays in quartz but

despite these results they proved the aptitude for the use of these excessively degreaser clays for the manufacture of Ceramic bricks with mixtures.

The silica contents (SiO_2) are within the desirable range as ceramic raw material, not exceeding 60wt.% (Tab.1). The concentrations of alkaline oxides (Na_2O and K_2O) are relatively low and consistent with the contents of illite and absence of fluxing agents such as feldspars. The iron oxides and hydroxides contents in the Tabarka clays are very low (0.01 to 1.14 wt. %) in comparison to Sejnane clays (5.5 to 7.6 wt. % of Fe_2O_3). This could generate white ceramic product. The total loss on ignition is relatively high in the Tabarka samples (10.78%) compared to the Sejnane samples (9.77%). This loss on ignition is dependent on the decomposition of clay minerals (kaolinite), the removal of absorbed and crystalline water and the alkali content. The high loss on ignition detected in RGS carbonate clay is 14.35%, it is due to the decomposition of kaolinite and carbonates.

The particle size distribution curves of the clays studied show similar shapes for both Tabarka and Sejnane clays. According to the particle size distribution curves, the fraction less than 2 μm is large about 63 -70% for S8 and S9 while O1 and O4 are on the order of 53 to 63%. The high fraction contents below 2 μm is closely related to the mineralogical composition rich in kaolinite. The coarse silty and sandy fractions are then important. These results are in perfect correlation with the mineralogy of clays. The study of these particle size curves as well as the Bigot curves reveal the quantities of sand to be added to the mixture used for the manufacture of ceramic tiles. The particle size distribution curve of the added sand shows a coarse fraction not exceeding 300 μm . its medium sized sand fig. 4).

The drying behavior can be deduced from the Bigot curves (Fig. 5). These clays have a relatively high drying shrinkage (around 5%) consistent with the plasticity values. The drying behavior is a parameter used in the ceramic industry as the prime indicator for selection of the raw material (Dondi et al., 1998, Meseguer, 2010). This behavior is deduced from the Bigot curves. According to the curves, we notice a total mass loss of 20.8% for the Tabarka clays and 25.5% for the Sejnane clays. This loss of mass is characterized by two stages. The first mass loss consists of the colloidal water loss which is 14.61% for the Tabarka clays and 10.07% for that of Sejnane. This proves that the latter are characterized by a faster drying than Tabarka clays. The second loss of mass is linked to the departure of the interposition water which are 6.19% and 15.45% respectively for S9 and O1. According to these results, Tabarka clays have a slow drying behavior which suggests the addition of a degreaser.

According to the particle size distribution curves, Tabarka clays are finer than Sejnane clays and therefore require a significant amount (15%) of sand as a degreaser. however only 5% of sand has been added to Sejnane clays and this is to avoid faults during drying and firing and to ensure good resistance to bending. The thermal behavior of these Numidian clays is reported in Figure 6. The water of hydration in the interlayer space disappeared at a temperature between 60 and 100°C. An endothermic peak on the DTA curve appears around the same temperatures. At 550°C, the expulsion of constitution water dehydroxylation is depicted by a second major endothermic peak. At this stage, the mass loss is between 8 and 10%, which is in accordance with the LOI (Table 1).

Formulations of the ceramic tiles are reported in Table 2. The Tabarka samples S8 and S9 show the similar expansion behavior with a total shrinkage of 0.66% and 1.05% for S8 and S9, respectively (Table 3, Fig. 7). A higher shrinkage is recorded on the Sejnane

samples due to the richness in melting (sum Fe_2O_3 , MgO , CaO , Na_2O and K_2O equal to 11%) compared to Tabarka clays (4%). These fluxes tend to promote vitrification and increase shrinkage (Tite et Maniatis, 1975, in Cultrone et al., 2001).

Concerning the bending strength, the values increase with temperature but do not exceed 5.3MPa (table 3) and are below the required standards of ceramic wall tiles (ISO 10545-4, 2004). As a consequence, various corrections in compositional mixtures were implemented to improve the mechanical strength, as discussed below.

The values of the drying shrinkage are of the order of 1.11% and 0.21% for ceramic tiles obtained from S8 and S9, respectively, and 1.55 and 1.47 for O1 and O4. These values are relatively high and should be minimized using the silica sand addition. The water absorption classifies these products in the BIII group of international standards (ISO 13006) with the exception of products O1 and O4 fired at 1150°C that belong to the BII group.

Compared to previous compositions (made exclusively of crude clays), the mixture products inhibited lower drying shrinkages close to 0.5 % (Table3). The firing shrinkage is lower than 2.5%. A good pressure (250- 280bars) applied to the tiles at a 6-7% humidity rate helped to avoid the lamination problems (Padoa, 1982). The bending strengths range from 13 to 16 N/mm^2 and are considered as close to the international standards for wall tiles requirements (15MPa) (Table3). This criterion reflects a good densification of the ceramics tiles. In comparison with the values of parameters of the crude products (Table 3), the results of the various parameters of the ceramics tiles resulting from the mixtures show a significant improvement. The water absorptions, ranging from 10.98% to 14.48% (Fig.8), classify these products as group BIII (ISO 13006- and NF EN ISO 10545-3). The Figure 9 shows the relationship between water

absorption and firing shrinkage. The intersection of both curves allows at choosing the optimum temperatures for firing these products in order to minimize the processing costs. According to these observations, it obvious that the Tabarka products require higher firing temperatures (1120 to 1150°C). These temperatures are close to the sanitary ware ceramic firing temperatures, and consequently these clays can constitute a good raw material for these applications. For Sejnane based products, the firing temperature should be lower (about 1020°C). These ceramic tiles are dark red colored and present a good quality aspect.

The firing transformations are represented by X-ray diffraction in figures 9 and 10. The X-ray diffractions of the raw mixtures before firing are compared with those fired at 1000, 1050, 1100 and 1150 °C. The crude mixtures show the richness in Kaolinite and in illite in the presence of quartz. According to DTA, the kaolinite disappears at 550°C, on the other hand from 1000°C (both case of MO1 1000 and S8 1000) the amount of illite decreases to disappear at 1050 ° C. From 1100 ° C, the beginning of the formation of mullite is recorded (reference code: 2-431) marked by the peak at 5.39Å. Mullite is an important ceramic material because of its low density, high thermal stability, and stability in severe chemical environments (Cao et al., 2004). For a higher temperature (1150 °C), a peak at 4.06Å only for fired products of Tabarka records the formation of cristobalite (reference code 1-76-939). A peak at 2.94Å appears on the X-rays diffractograms of the all fired product of Tabarka and Sejnane attributed to the formation of the diopside (reference code 1-83-1820). The Sejnane clays are rich in iron oxide (Table 1). These iron oxides contributed to the formation of hematite (Fig.10) recorded only on fired products of Sejnane and marqued by a peak at 2.69Å (code reference 1-1053) which ensures a certain rigidity of the ceramics tiles (high bending strength), due to its fluxing character. The quartz initially present in the mixtures of raw

clays persists during all firing phases. The presence of silicon, alkaline and calco-alkali compounds support the formation of plagioclases (albite and anorthite) (Lee et al., 2008) which appear from 1000 ° C but their quantities increase depending on the temperature.

Few pores are visible on the SEM observations (Fig.11). At the temperature of 1050°C and 1100°C, these materials show the same crystalline structure with the presence of siliceous glass. The SEM observation of ceramic tiles MO1 reveal the presence of significant amount of glassy phase. The quartz occupies the voids between the particles.

These products can be judged of good quality because of their good technological characteristics and appearance. There are no major defects detected during drying and firing. Defects revealed upon the use of raw clay were corrected by the addition of sand and feldspar. The addition of carbonated clay reduced the firing temperatures. Carbonated clay (RGS) was added (20%) in all mixtures with the aim of increasing the CaO content and promoting the formation of a glassy phase (Kazmi et al., 2017) because these crude clays have a low CaO content (table 1). Moreover, the presence of calcite, dolomite or both can influence the formation of different minerals at high temperatures (Trindade et al., 2010). The presence of fluxing oxides including Fe₂O₃ tend to reduce the temperature at which a partial melt is formed (Abdelmalek et al., 2017). The iron oxide is the main colorant in clayey materials, responsible for the reddish color observed after firing (Abajo, 2000 in Abdelmalek et al., 2017).

These materials can be considered as refractory because of its high content in kaolinite and sand (Hachani et al., 2012). Therefore, these Oligocene clays of northern Tunisia can be a good raw material for the manufacture of ceramic tiles. The clays of Tabarka can be used in the production of sanitary ceramics due to their fine clay particles and

their good densification during firing at high temperatures. These trials made in the laboratory must be supplemented with other mixtures of clays and on an industrial scale to confirm their ability to be a good raw material for ceramics.

Conclusion

The Tabarka and Sejnane clays, which belong to the Numidian Flysch, whose thicknesses can reach 3000 meters, were studied in order to decipher their use in ceramic manufacturing. The characterization of the raw clays shows a mineralogy composition dominated by kaolinite and illite and relatively high quartz content for the two sites of Tabarka and Sejnane. Chemical analyzes show a significant richness in SiO_2 ; this can be explained by the presence of clays and silica sand. The mineralogical and chemical results are consistent. According to the particle size distribution curves, the Sejnane clays have a larger coarse particle size fraction compared to those of Tabarka which influences the percentage of sand additions as degreaser. These clays were tested in the manufacture of ceramic tiles. Technological tests show the aptitude of these raw materials to be used in the manufacture of ceramic tiles on an industrial scale. The aspect of ceramic tiles is acceptable with characteristics close to the required standards. In particular, the drying and firing shrinkages are low, the flexural strength and the water absorption are also within the standard limits. Tabarka ceramic tiles have a white color due to the richness in kaolinite and the rarity of iron oxides. These clays can be used as raw materials for ceramic tiles. Sejnane ceramic tiles have a red color due to the richness of iron oxide initially present in raw clays. These very abundant Numidian clays alternate in succession with metric, sometimes decametric, levels of consolidated sandstone. These geological outcrops extended to the northwest of Tunisia

in the Tellian domain, present immense geological deposits of industrially useful raw material.

Acknowledgment

This research was financed by the Ministry of Higher Education, Scientific Research and Technology (Tunisia), and the Belgian-Tunisian project “Valorisation des argiles” of the Wallonie-Bruxelles International (WBI). Thanks are due for the support of the CTMCCV (Centre Techniques de Matériaux de Construction de Céramique et du Verre Tunis - Tunisie).

References

- Abajo, M.F., 2000. Manual sobre fabricación de baldosas, tejas y ladrillos. Ed. Beralmar S. A., (Barcelona).
- Abdelmalek, B., Rehia, B., Youcef, B., Lakhdar, B., Nathalie, F., (2017). Mineralogical characterization of Neogene clay areas from the Jijel basin for ceramic purposes (NE Algeria -Africa). *Applied Clay Science*, 136, 176–183. doi:10.1016/j.clay.2016.11.025.
- Abidi R., Slim-Shimi N., Somarin A., Henchiri M., (2010). Mineralogy and fluid inclusions study of carbonate-hosted Mississippi valley-type Ain AllegaPb–Zn–Sr–Ba ore deposit, Northern Tunisia. *Journal of African Earth Sciences* 57, (2010) 262–272. <https://doi.org/10.1016/j.jafrearsci.2009.08.006>
- Baccour H., Medhioub M., Jamoussi F., & Mhiri T. (2009). Influence of firing temperature on the ceramic properties of Triassic clays from Tunisia. *Journal of Materials Processing Technology*, 209(6), 2812–2817. doi:10.1016/j.jmatprotec.2008.06.055
- Ben M’barek Jemaï M., Sdiri A., Errais E., Duplay J., Ben Saleh I., Zagarni M. F., & Bouaziz S. (2015). Characterization of the Ain Khemouda halloysite (western Tunisia) for ceramic industry. *Journal of African Earth Sciences*, 111, 194–201. doi:10.1016/j.jafrearsci.2015.07.014
- Ben Salah I., M’barek Jemaï M. B., Sdiri A., Boughdiri M., & Karoui N. (2016). Chemical and technological characterization and beneficiation of Jezza sand (North West of Tunisia): Potentialities of use in industrial fields. *International Journal of Mineral Processing*, 148, 128–136. doi:10.1016/j.minpro.2016.01.016

411 Ben Salah I., Sdiri A., Ben M'barek Jemai M., & Boughdiri M. (2018). Potential use of
 412 the lower cretaceous clay (Kef area, Northwestern Tunisia) as raw material to
 413 supply ceramic industry. *Applied Clay Science*, 161, 151–162.
 414 doi:10.1016/j.clay.2018.04.015

415 Bennour A., Mahmoudi S., & Srasra E. (2017). Physico-chemical and geotechnical
 416 characterization of Bargou clays (Northwestern Tunisia): application on traditional
 417 ceramics. *Journal of the Australian Ceramic Society*, 54(1), 149–159.
 418 doi:10.1007/s41779-017-0136-5

419 Bennour A., Mahmoudi S., Srasra E., Boussen S., & Htira N. (2015). Composition,
 420 firing behavior and ceramic properties of the Sejnène clays (Northwest Tunisia).
 421 *Applied Clay Science*, 115, 30–38. <https://doi.org/10.1016/j.clay.2015.07.025>

422 Bouaziz S., Barrier E., Soussi M., Turki M. M., Zouari H., (2002). Tectonic evolution
 423 of the northern African margin in Tunisia from paleostress data and sedimentary
 424 record. *Tectonophysics*, 357, (2002) 227-253. [https://doi.org/10.1016/S0040-](https://doi.org/10.1016/S0040-1951(02)00370-0)
 425 [1951\(02\)00370-0](https://doi.org/10.1016/S0040-1951(02)00370-0)

426 Boussen S., Sghaier D., Chaabani F., Jamoussi B., & Bennour A. (2016).
 427 Characteristics and industrial application of the Lower Cretaceous clay deposits
 428 (Bouhedma Formation), Southeast Tunisia: Potential use for the manufacturing of
 429 ceramic tiles and bricks. *Applied Clay Science*, 123, 210–221.
 430 doi:10.1016/j.clay.2016.01.027

431 Cao X. Q., Vassen R., Stoeber D., (2004). Ceramic materials for thermal barrier
 432 coatings. *Journal of the European Ceramic Society* 24, (2004) 1–10.
 433 [https://doi.org/10.1016/S0955-2219\(03\)00129-8](https://doi.org/10.1016/S0955-2219(03)00129-8)

434 Chihi R., Blidi I., Trabelsi-Ayadi M., & Ayari F. (2019). Elaboration and
 435 characterization of a low-cost porous ceramic support from natural Tunisian
 436 bentonite clay. *Comptes Rendus Chimie*. doi:10.1016/j.crci.2018.12.002

437 Crampon N., (1973). L'extrême nord tunisien. Aperçu stratigraphique, pétrologie et
 438 structural. Livre jubilaire M. Solignac. *Ann. Min. et Géol. Tunis.*; 26, pp. 49–85.

439 Decrée S., De Putter T., Yans J., Moussi B., Recourt P., Jamoussi F., Bruyère D. &
 440 Dupuis C., (2008). Iron mineralization in marginal basins surrounding Fe-Pb-Zn
 441 sulphide deposits (Neogene Tunisian Tell, Nefza district): mixed influence of
 442 pedogenesis and hydrothermal alteration. *Ore Geology Reviews* 33, 3-4, 397-410.
 443 <https://doi.org/10.1016/j.clay.2018.07.007>

444 Decrée S., Marignac C., Liégeois J. P., De Putter T., Yans J., Ben Abdallah R.,
 445 Demaiffe D., (2014). Miocene magmatic evolution in the Nefza District (Northern
 446 Tunisia). *Lithos* 192-195, 240-258. <https://doi.org/10.1016/j.lithos.2014.02.001>

447 Dondi, M., Marsigli, M., Ventura, I., 1998. Sensibilità all'esiccamento e caratteristiche
 448 porosimetriche delle argille italiane per laterizi. *Ceramurgia* 28, 1–8.

449 Felhi M., Tlili A., Gaied M. E., Montacer M., (2008). Mineralogical study of kaolinitic
 450 clays from Sidi El Bader in the far north of Tunisia. *Applied Clay Science* 39 p208–
 451 217.

452 Fildes C., Stow D.A.V., Riahi S., Soussi M., Patel U., Milton J.A., Marsh S., (2009).
 453 European Provenance of the Numidian Flysch in northern Tunisia. *Terra Nova*, Vol
 454 22, No. 2, 94–102. <https://doi.org/10.1111/j.1365-3121.2009.00921.x>

455 Frizon de Lamotte D., Saint-Bezar B., Bracene R., Mercier E., (2000). The two main
 456 steps of the Atlas building and geodynamics of the western Mediterranean.
 457 Tectonics, 19, 740–761. <https://doi.org/10.1029/2000TC900003>

458 Grabowska-Olszewska B., (2003). Modelling physical properties of mixtures of clays:
 459 example of two component mixture of kaolinite and montmorillonite. Applied Clay
 460 Science, 22, 251-259. [https://doi.org/10.1016/S0169-1317\(03\)00078-4](https://doi.org/10.1016/S0169-1317(03)00078-4)

461 Guerrera F., Martin-Algarra A., Perrone V., (1993). Late Oligocene-Miocene syn-late-
 462 orogenic successions in western and central Mediterranean chains from the Betic
 463 Cordillera to the Southern Apennines: Terra, Nova, 5, 525–544.
 464 <https://doi.org/10.1111/j.1365-3121.1993.tb00302.x>

465 Hachani M., Hajjaji W., Moussi B., Medhioub M., Rocha F., Labrincha J. A., &
 466 Jamoussi F. (2012). Production of ceramic bodies from Tunisian Cretaceous clays.
 467 Clay Minerals, 47(01), 59–68. doi:10.1180/claymin.2012.047.1.59

468 Hajjaji W., Moussi B., Hachani M., Medhioub M., Lopez-Galindo A., Rocha F.,
 469 Jamoussi F. (2010). The potential use of Tithonian–Barremian detrital deposits from
 470 central Tunisia as raw materials for ceramic tiles and pigments. Applied Clay
 471 Science, 48(4), 552–560. doi:10.1016/j.clay.2010.03.003

472 Hammami-Ben Zaied F., Abidi R., Slim-Shimi N., & Somarin A. K. (2015). Potentiality
 473 of clay raw materials from Gram area (Northern Tunisia) in the ceramic industry.
 474 Applied Clay Science, 112-113, 1–9. doi:10.1016/j.clay.2015.03.027

475 Hedfi I., Hamdi N., Rodriguez M. A., & Srasra E. (2016). Development of a low cost
 476 micro-porous ceramic membrane from kaolin and Alumina, using the lignite as

477 porogen agent. Ceramics International, 42(4), 5089–5093.
478 doi:10.1016/j.ceramint.2015.12.023

479 Hedfi I., Hamdi N., Srasra E., & Rodríguez M. A. (2014). The preparation of micro-
480 porous membrane from a Tunisian kaolin. *Applied Clay Science*, 101, 574–578.
481 doi:10.1016/j.clay.2014.09.021

482 Holtz, R.D., Kovacs, W.D., 1981. *An Introduction to Geotechnical Engineering*.
483 Prentice-Hall, Englewood Cliffs, New Jersey.

484 Hoyez, B., (1975). Dispersion du matériel quartzeux dans les formations aquitaniennes
485 de Tunisie septentrionale et d’Algérie nord-orientale. *Bull. Soc. Géol. Fr.*, XVII :
486 1147-1156.

487 ISO 10545-3, (1995). *Ceramic tiles. Part 3: Determination of water absorption, apparent*
488 porosity, apparent relative density and bulk density. Edition 1.

489 ISO 10545-4, (2004). *Ceramic tiles. Part 4: Determination of modulus of rupture and*
490 breaking strength. Edition 2.

491 ISO 13006, (2012). *Carreaux et dalles céramiques — Définitions, classification,*
492 caractéristiques et marquage.

493 Jemmali N., Souissi F., Carranza E. J. M., Vennemann T. W., (2013). Mineralogical and
494 Geochemical Constraints on the Genesis of the Carbonate-Hosted Jebel Ghazlane
495 Pb-Zn Deposit (Nappe Zone, Northern Tunisia). *Resource Geology* Volume 63,
496 Issue 1, January 2013, Pages 27-41. doi: 10.1111/j.1751-3928.2012.00208.x

497 Jemmali N., SouissiF., Villa I. M., Vennemann T. W., (2011). Ore genesis of Pb-Zn
498 deposits in the Nappe zone of Northern Tunisia: Constraints from Pb-S-C-O isotopic

499 systems. *Ore Geology Reviews* Volume 40, Issue 1, September 2011, Pages 41-53.
500 doi.org/10.1016/j.oregeorev.2011.04.005

501 Jeridi K., Hachani M., Hajjaji W., Moussi B., Medhioub M., Lopez-Galindo A., Kooli
502 F., Zargouni F., Labrincha J.A. & Jamoussi F., (2008). Technological behaviour of
503 some Tunisian clays prepared by dry ceramic processing. *Clay Minerals*, 43, 339-
504 350. DOI: 10.1180/claymin.2008.043.3.01

505 Jeridi K., López-Galindo, A., Setti M., Jamoussi F., (2014). The use of Dynamic
506 Evolved Gas Analysis (DEGA) to resolve ceramic defects. *Applied Clay Science*,
507 Volume 87, January 2014, Pages 292-297.
508 <https://doi.org/10.1016/j.clay.2013.10.021>

509 Jolivet L., and Faccenna C., (2000). Mediterranean extension and the African-Eurasia
510 collision. *Tectonics*, 19, 1095–1106. <https://doi.org/10.1029/2000TC900018>

511 Jordan M. M., Boix A., Sanfeliu T., De la fuente C., (1999). Firing transformations of
512 cretaceous clays used in the manufacturing of ceramic tiles, *Appl. Clay Sci.* 14, pp.
513 225-234. [https://doi.org/10.1016/S0169-1317\(98\)00052-0](https://doi.org/10.1016/S0169-1317(98)00052-0)

514 Kamoun N., Jamoussi F., & Rodríguez M. A. (2019). The preparation of meso-porous
515 membranes from Tunisian clay. *Boletín de La Sociedad Española de Cerámica y*
516 *Vidrio*. doi:10.1016/j.bsecv.2019.06.001

517 Kazmi S.M., Abbas S., Nehdi M.L., Saleem M.A., Munir M.J., (2017). Feasibility of
518 using waste glass sludge in production of ecofriendly clay bricks. *J. Mater. Civ.*
519 *Eng.* 29, 4017056. DOI: 10.1061/(ASCE)MT.1943-5533.0001928

520 Khemakhem S., Larbot A., & Ben Amar R. (2009). New ceramic microfiltration
 521 membranes from Tunisian natural materials: Application for the cuttlefish effluents
 522 treatment. *Ceramics International*, 35(1), 55–61.
 523 doi:10.1016/j.ceramint.2007.09.117

524 LCPC, (1987). Limites d'Atterberg, limite de liquidité, limite de plasticité. Méthode
 525 d'essai n°19, Laboratoire Central des Ponts et Chaussées, 26 pp.

526 Lee W.E., Souza G.P., McConville C.J., Tarvornpanich T., Iqbal Y., (2008). Mullite
 527 formation in clays and clay-derived vitreous ceramics. *Journal of the European*
 528 *Ceramic Society* 28 - 465–471. <https://doi.org/10.1016/j.jeurceramsoc.2007.03.009>

529 López-Galindo A., Torres-Ruiz J. & Gonzalez-López J.M., (1996). Mineral
 530 quantification in sepiolite-palygorskite deposits using X-ray diffraction and
 531 chemical data. *Clay Minerals*, 31, 217-224. DOI:
 532 <https://doi.org/10.1180/claymin.1996.031.2.07>

533 Mahmoudi S., Bennour A., Srasra E., & Zargouni F. (2016). Determination and
 534 adjustment of drying parameters of Tunisian ceramic bodies. *Journal of African*
 535 *Earth Sciences*, 124, 211–215. doi:10.1016/j.jafrearsci.2016.09.031

536 Mahmoudi S., Bennour A., Srasra E., & Zargouni F. (2017). Characterization, firing
 537 behavior and ceramic application of clays from the Gabes region in South Tunisia.
 538 *Applied Clay Science*, 135, 215–225. doi:10.1016/j.clay.2016.09.023

539 Medhioub M. , Baccour H., Jamoussi F., Mhiri T. (2010). Composition and ceramic
 540 properties of triassic clays from Tunisia. *Journal of Ceramic Processing*
 541 *Research* Volume 11, Issue 2, 2010, Pages 209-214

542 Medhioub M., Hajjaji W., M. Hachani, Lopez-Galindo A., Rocha F., Labrincha J.A.
 543 &Jamoussi F. , (2012). Ceramic Tiles Based On Central Tunisian. Clays (SidiKhalif
 544 Formation), Clay Minerals, (2012) 47, 165–175. DOI: [https:// doi.org/10.1180/](https://doi.org/10.1180/claymin.2012.047.2.02)
 545 claymin. 2012.047.2.02

546 Meseguer S., Sanfeliu T., Jordan M.M. , (2009). Classification and statistical analysis of
 547 mine spoils chemical composition from Oliete Basin (Teruel. NE Spain).
 548 Environmental Geology 56, 1461–1466. DOI:10.1007/s00254-008-1241-0

549 Meseguer, S., 2010. Ceramic behaviour of five Chilean clays which can be used in the
 550 manufacture of ceramic tile bodies. Appl. Clay Sci. 47, 372–377.
 551 <https://doi.org/10.1016/j.clay.2009.11.056>

552 Moussi B., 2012. Thèse de doctorat en sciences géologique . Mode de genèse et
 553 valorisation de quelques argiles de la région de Nefza-Sejnane (Tunisie
 554 Septentrionale)., Université de Carthage, Tunisie .157p.

555 Moussi B., Medhioub M., Hatira N., Yans J., Hajjaji W., Rocha F., Labrincha J.A.
 556 &Jamoussi F. , (2011). Identification and use of white clayey deposits from the area
 557 of Tamra (Northern Tunisia) as ceramic raw materials. Clay Minerals, (2011) 46,
 558 165–175. <https://doi.org/10.1180/claymin.2011.046.1.165>

559 Padoa L., (1982). La cottura dei prodotti ceramici. Terza Edizione, Faenza Editrice,
 560 Italy. 299 pp.

561 Parize O., Beaudoin B., Burollet P.F., Cojan G., Fries G., Pinault M., (1986). La
 562 provenance du matériel gréseux numidien est septentrionale (Sicile et Tunisie). C.R.
 563 Acad. Sci. Paris, 18: 1671-1674.

564 Riahi S., Soussi M., Boukhalfa K. Ben Ismail Lattrache K, Dorrik S., Khomsi S., Bedir
 565 M., (2010). Stratigraphy, sedimentology and structure of the Numidian Flysch thrust
 566 belt in northern Tunisia. *Journal of African Earth Science* 57 (109–126).
 567 <https://doi.org/10.1016/j.jafrearsci.2009.07.016>

568 Rouvier H., (1977). *Géologie de l'extrême Nord-Tunisien: tectonique et*
 569 *paléogéographie superposées à l'extrémité orientale de la chaîne Nord-Maghrebine.*
 570 *Thèse de doctorat, Université Pierre et Marie Curie (Paris, France), 215p.*

571 Rouvier H., (1994). Notice explicative de la carte géologique de la Tunisie au 1/50000e
 572 – Nefza, feuille 10. Office National des Mines, Direction de la Géologie, 48p.

573 Sghaier D., Chaabani, F., Proust D., Vieillard P., (2014). Mineralogical and
 574 geochemical signatures of clays associated with rhyodacites in the Nefza area
 575 (northern Tunisia). *Journal of African Earth Sciences* Volume 100, December 2014,
 576 Pages 267-277. <https://doi.org/10.1016/j.jafrearsci.2014.06.024>

577 Talbi F., Melki F., Ben Ismail-Lattrache K., Alouani R., Tlig S., (2008). Le Numidien
 578 de la Tunisie septentrionale: données stratigraphiques et interprétation
 579 géodynamique. *Estudios Geol.*, Vol. 64, n.º 1, 31-44, enero-junio. ISSN: 0367-0449.

580 Talbi, F., (1998). Petrologie, géochimie, études des phases fluides et gîtologie liées au
 581 magmatisme néogène de la Tunisie septentrionale. *Thèse de doctorat. Université*
 582 *Tunis II.* 368 pp.

583 Torres-Ruiz J., López-Galindo A., González M., Delgado A., (1994). Geochemistry of
 584 Spanish sepiolite–palygorskite deposits: genetic considerations based on trace
 585 elements and isotopes. *Chemical Geology*, 112, 221-245.
 586 [https://doi.org/10.1016/0009-2541\(94\)90026-4](https://doi.org/10.1016/0009-2541(94)90026-4)

- Trindade, M.J., Dias, M.I., Coroado, J., Rocha, F., (2009). Mineralogical transformations of calcareous rich clays with firing: a comparative study between calcite and dolomite rich clays from Algarve, Portugal. *Appl. Clay Sci.* 42, 345–355. <http://doi.org/10.1016/j.clay.2008.02.008>.
- Wezel, F. C., (1970). Numidian Flysch: an Oligocene-Early Miocene continental rize deposit of the African platform. *Nature* 228, 275-276.
- Wildi, W., (1983). La chaîne tello-rifaine (Algérie, Maroc, Tunisie): structure, stratigraphie et évolution du Trias au Miocène. *Rev. Géol. Dyn. Géogr. Phys.*, 24: 201-297.
- Yaich C., Hooyberghs H.J.F., Durllet C., Renard M., (2000). Corrélation stratigraphique entre les unités oligo-miocènes de Tunisie centrale et le Numidien. *C.R. Acad. Sci. Paris*, 331, 499-506. [https://doi.org/10.1016/S1251-8050\(00\)01443-9](https://doi.org/10.1016/S1251-8050(00)01443-9)
- Zouaoui H., & Bouaziz J. (2017). Physical and mechanical properties improvement of a porous clay ceramic. *Applied Clay Science*, 150, 131–137. doi:10.1016/j.clay.2017.09.002

Table Captions

Table1. Mineralogical (%) and chemical (wt.%) compositions of the studied samples.

Table 2. Ceramic tiles formulations.

Tables 3. Technological parameters of obtained ceramic products.

Figure Captions

Fig.1. Parts of geological map of Nefza (1) and Oued Sejnane (2) on scale 1/50.000 (Western southern area) showing the localization of the studied sections of Sidi Bader and Om Tebal.

Fig.2. Lithological sections of (1) Sidi Bader in the Tabarka area and Om Tebal in Sejnane area (2) (Felhi et al.. 2008; modified).

Fig. 3. Representation of the studied samples. using the Holtz & Kovacs (1981) diagram.

Fig. 4. Particle size distribution of the four clayey samples and the sand used in the mixture.

Fig. 5. Bigot curves of some clayey samples.

Fig. 6. DTA-TG curves of samples O1 and S8.

Fig. 7. Dilatometric curves of the studied samples grouped by site.

Fig. 8. Variation of the firing shrinkage of the ceramics tiles and the water absorption.

Fig.9: XRD patterns of S8 clay and the ceramic tiles resulting from mixture MS8 fired at various temperatures (1000°C. 1050°C. 1100°C and 1150°C); Qz: quartz; He: hematite; Mu: mullite; Di: diopside; Kao: kaolinite; Ill: illite

Fig. 10: XRD patterns of O1 clay and the ceramic tiles resulting from mixture MO1 fired at various temperatures (1000°C. 1050°C. 1100°C and 1150°C); Al: albite; Qz: quartz; He: hematite; Mu: mullite; Di: diopside; Kao: kaolinite; Ill: illite.

Fig. 11: Scanning electron micrographs of tiles from mixtures MS8 and MO1.

Table1. Mineralogical (%) and chemical (wt.%) compositions of the studied samples.

Mineralogy (%)											
	I-S	Illite	Kaolinite	Quartz	Calcite	Siderite					
O1	7	2	44	36	0	11					
O4	0	23	52	25	0	0					
S8	0	29	37	34	0	0					
S9	0	11	52	37	0	0					
RGS	0	11	45	30	14	0					
Stat. dev.	3(%)	3(%)	3(%)	3(%)	3(%)	3(%)					
Chemical analysis (wt.%)											
	SiO ₂	Al ₂ O ₃	Fe ₂ O ₃	MnO	MgO	CaO	Na ₂ O	K ₂ O	TiO ₂	P ₂ O ₅	L.O.I
O1	59.42	17.94	7.58	0.01	1.65	0.53	1.01	0.16	0.78	0.13	9.77
O4	57.31	19.75	6.99	0.02	1.62	0.49	0.03	2.01	0.66	0.12	8.77
S8	57.73	26.33	1.82	0.002	0.56	0.27	0.09	2.2	1.32	0.46	10.52
S9	60.58	25.08	1.96	0.01	0.64	0.17	0.04	2.15	1.42	0.32	10.78
RGS	46.3	20.7	6.69	0.01	0.86	8.05	0.2	1.5	0.9	0.2	14.35
Stat. dev.	0.1	0.048	0.006	0.001	0.0072	0.012	0.017	0.017	0.0051	0.0074	

Stat. dev. :Standard deviation

659 Table 2. Ceramic tiles formulations.

	Clays (wt. %)					Sand (wt. %)	Feldspar (wt. %)
	S8	S9	O1	O4	RGS		
S8	100	-	-	-	0	0	0
S9	-	100	-	-	0	0	0
O1	-	-	100	-	0	0	0
O4	-	-	-	100	0	0	0
MS8	60	-	-	-	20	15	5
MS9	-	60	-	-	20	15	5
MO1	-	-	70		20	5	5
MO4	-	-	-	70	20	5	5

660

661

662

663

664

665

666

667

668

669

670

671

672

673

674

675

676

677

678 Table 3. Technological parameters of obtained ceramic products.

Raw	Firing shrinkage(%)				Water absorption(%)				Bending strength (N/mm ²)			
	S8	S9	O1	O4	S8	S9	O1	O4	S8	S9	O1	O4
Drying shr.	1.11	0.21	1.55	1.47	-	-	-	-	-	-	-	-
1000°C	0.93	0.23	0.9	0.53	19.42	13.87	13.07	15.41	0.95	0.65	2.24	0.97
1050°C	1.32	0.3	1.74	1.49	15.72	13.74	14.12	14.78	1.12	0.87	2.58	1.59
1100°C	1.54	0.78	3.29	1.55	14.82	12.17	11.2	14.63	1.29	1.31	4.06	3.07
1150°C	1.82	0.64	4.42	5.73	13.76	13.27	9.13	8.38	1.46	1.25	2.95	5.31
Stat. dev.	0.02	0.02	0.02	0.02	1	1	1	1	0.02	0.02	0.02	0.02
Mixtures	MS8	MS9	MO1	MO4	MS8	MS9	MO1	MO4	MS8	MS9	MO1	MO4
Drying shr.	0.02	0.19	0.42	0.54	-	-	-	-	-	-	-	-
1000°C	0.44	0.30	1.15	1.10	14.47	12.93	13.79	13.62	13.17	13.16	14.63	14.66
1050°C	0.74	0.53	1.77	1.64	14.47	12.53	12.43	12.33	13.28	13.36	15.63	15.56
1100°C	1.21	0.55	1.98	1.80	14.10	12.13	11.86	12.68	13.69	13.5	15.07	15.22
1150°C	2.00	1.02	2.14	2.54	11.95	11.48	10.98	11.47	15.31	13.66	15.95	15.67
Stat. dev.	0.02	0.02	0.02	0.02	1	1	1	1	0.02	0.02	0.02	0.02

679 Drying shr : Drying Shrinkage; Stat. dev. :Standard deviation

680

681

682

683

684

685

686

687

688

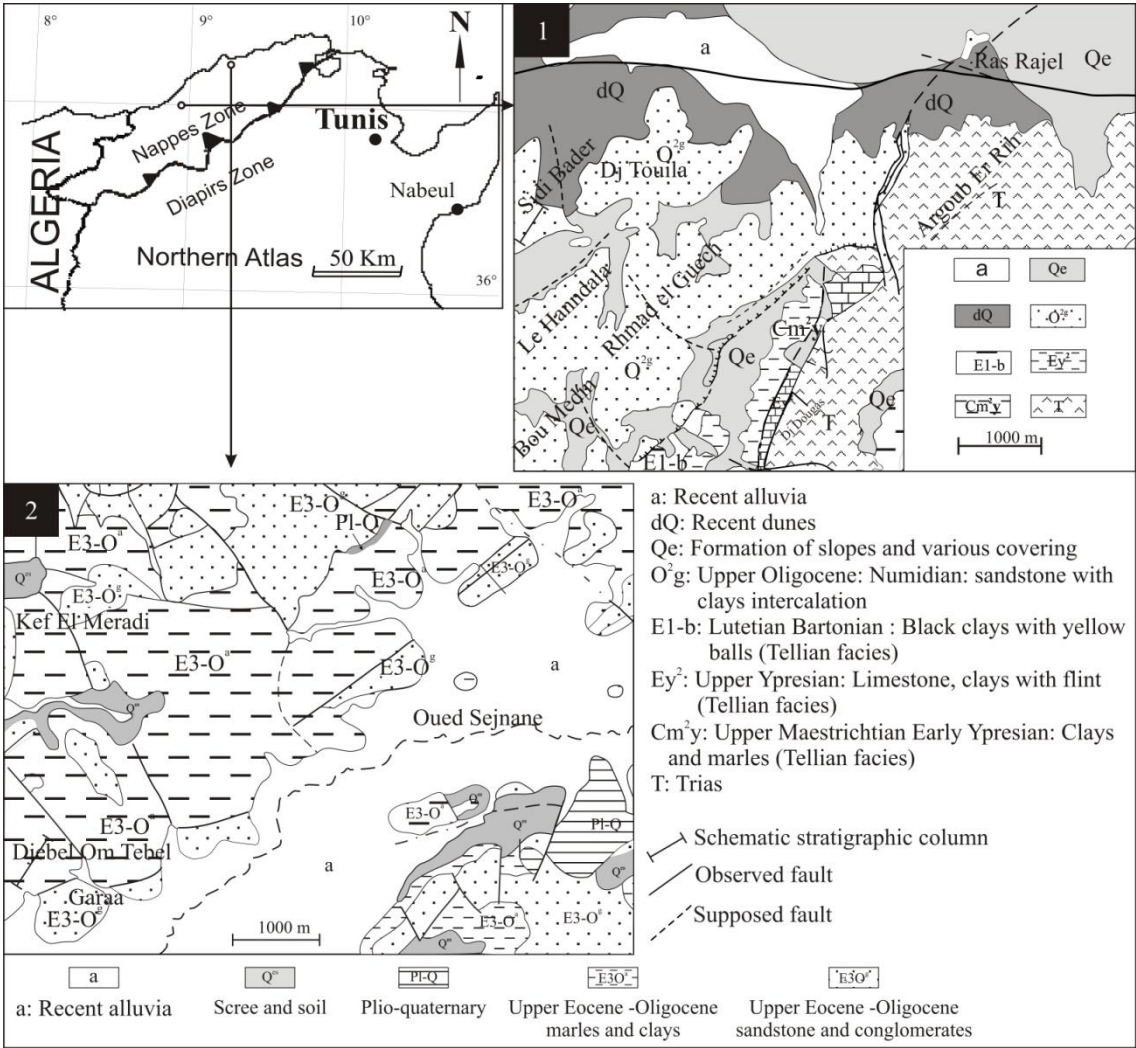
689

690

691

692

693 Fig. 1



694

695 Fig.1. Parts of geological map of Nefza (1) and Oued Sejnane (2) on scale 1/50.000
696 (Western southern area) showing the localization of the studied sections of Sidi Bader
697 and Om Tebal.

698

699

700

701

702

703

Fig. 2

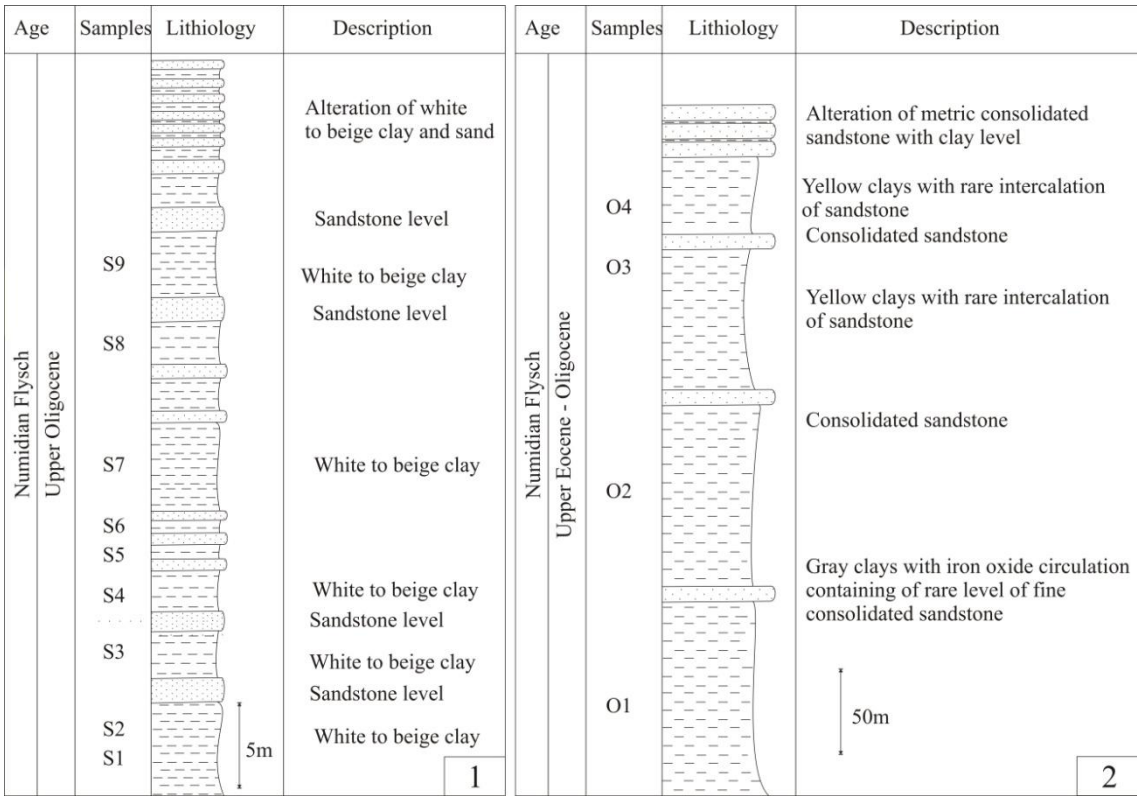


Fig.2. Lithological sections of (1) Sidi Bader in the Tabarka area and Om Tebal in Sejnane area (2) (Felhi et al.. 2008; modified).

Fig. 3

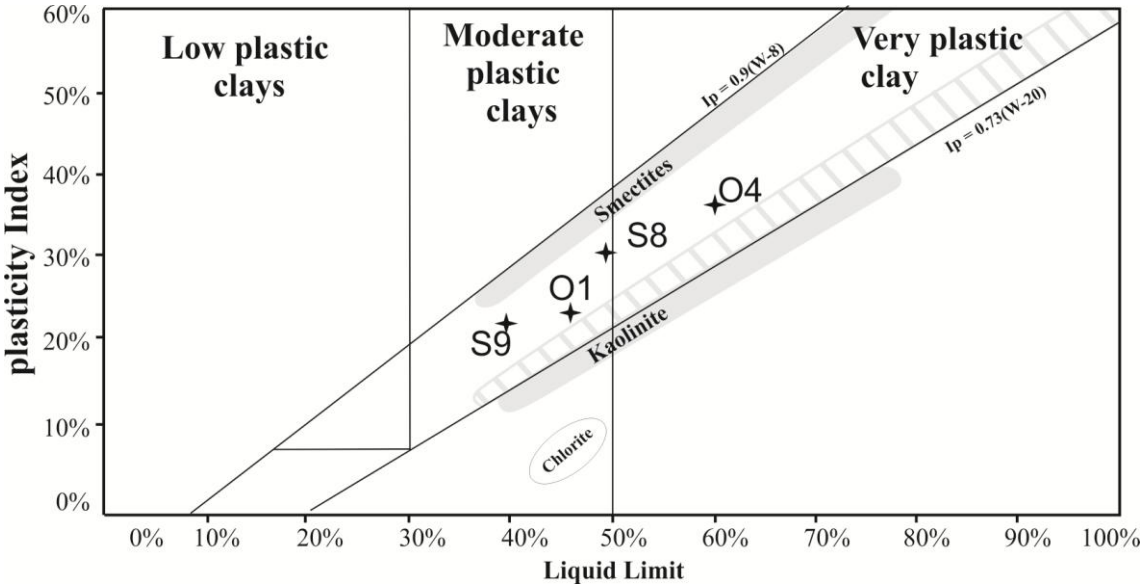


Fig. 3. Representation of the studied samples. using the Holtz & Kovacs (1981) diagram.

Fig. 4

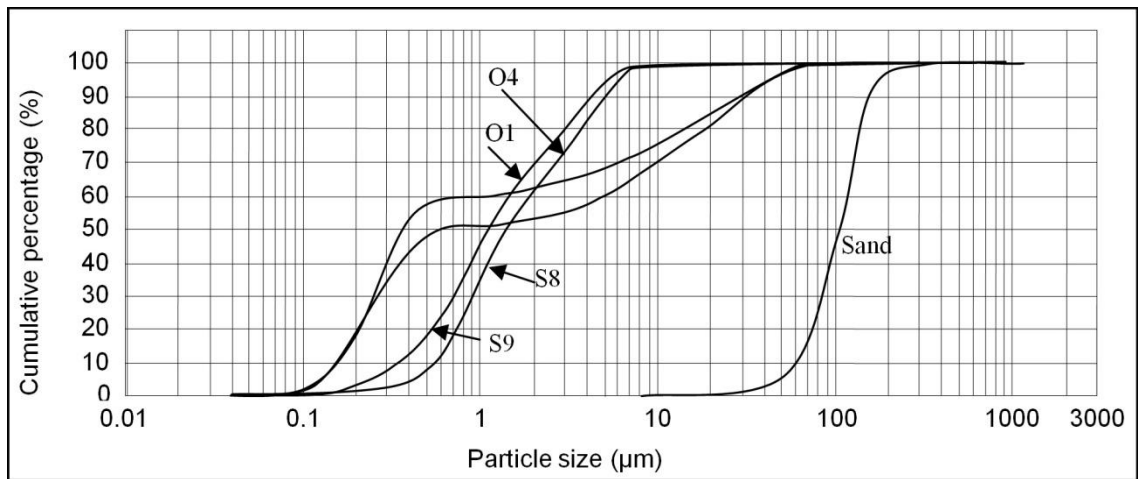


Fig. 4. Particle size distribution of the four clayey samples and the sand used in the mixture.

Fig. 5

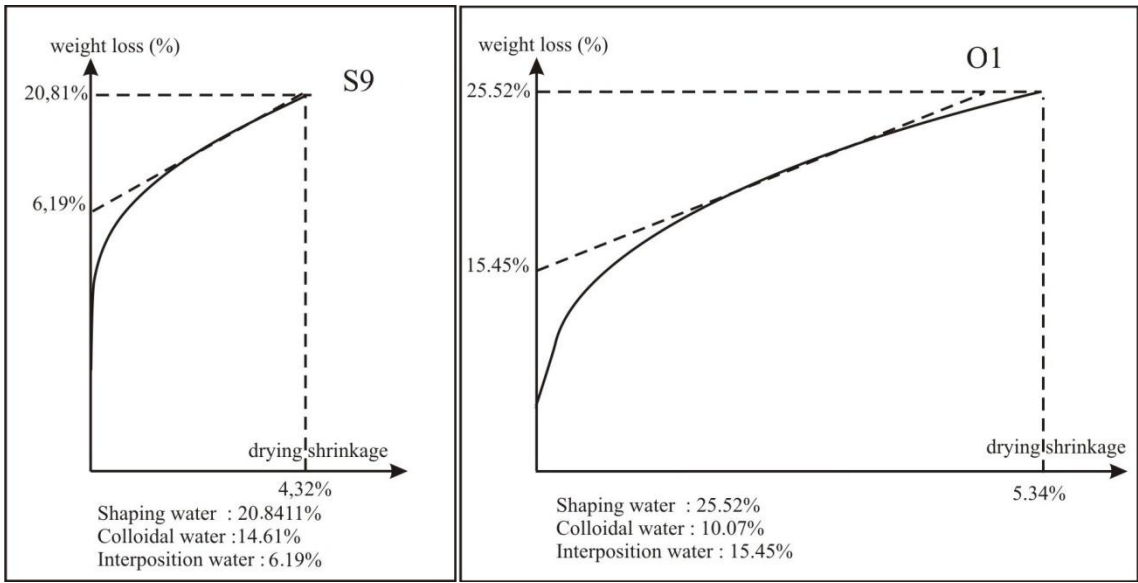


Fig. 5. Bigot curves of some clayey samples.

Fig. 6

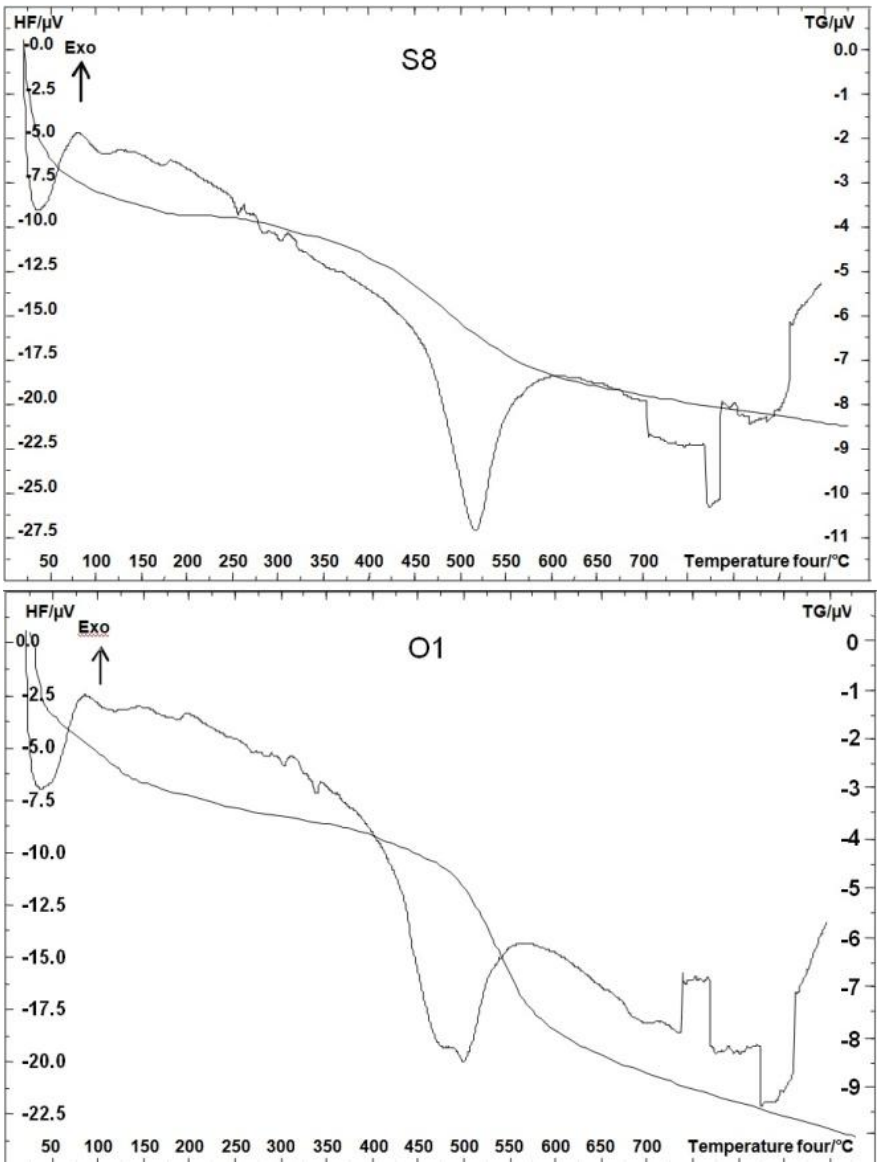


Fig. 6. DTA-TG curves of samples O1 and S8.

Fig. 7

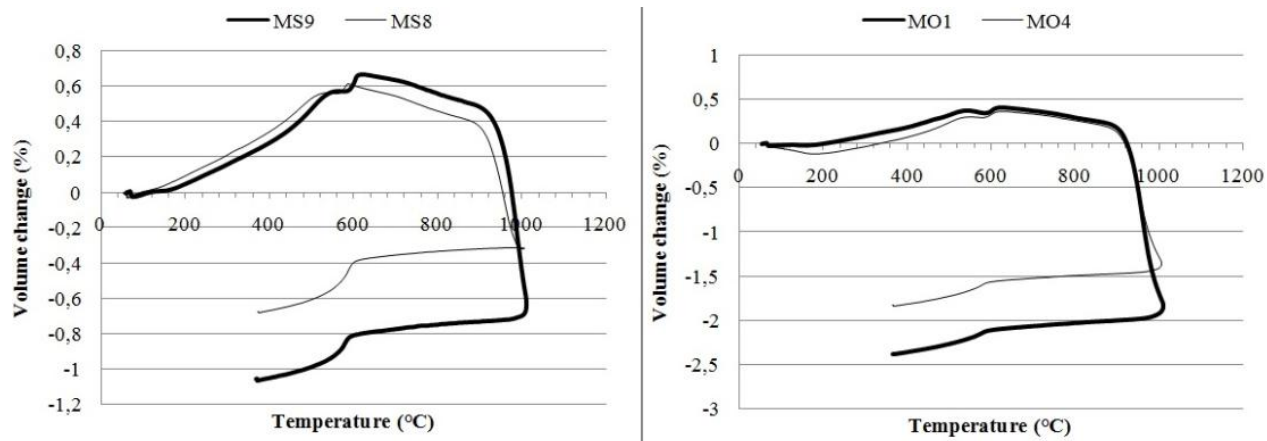
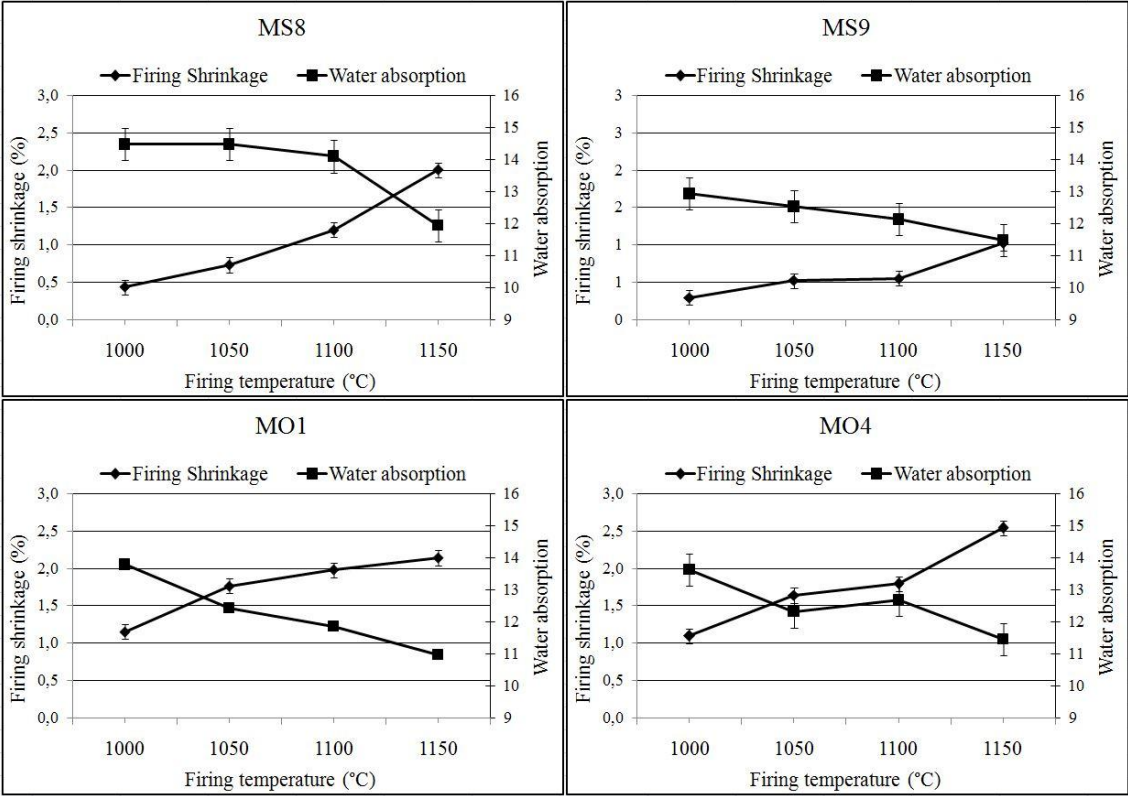


Fig. 7. Dilatometric curves of the studied samples grouped by site.

801 Fig. 8



802

803 Fig. 8. Variation of the firing shrinkage of the ceramics tiles and the water absorption.

804

805

806

807

808

809

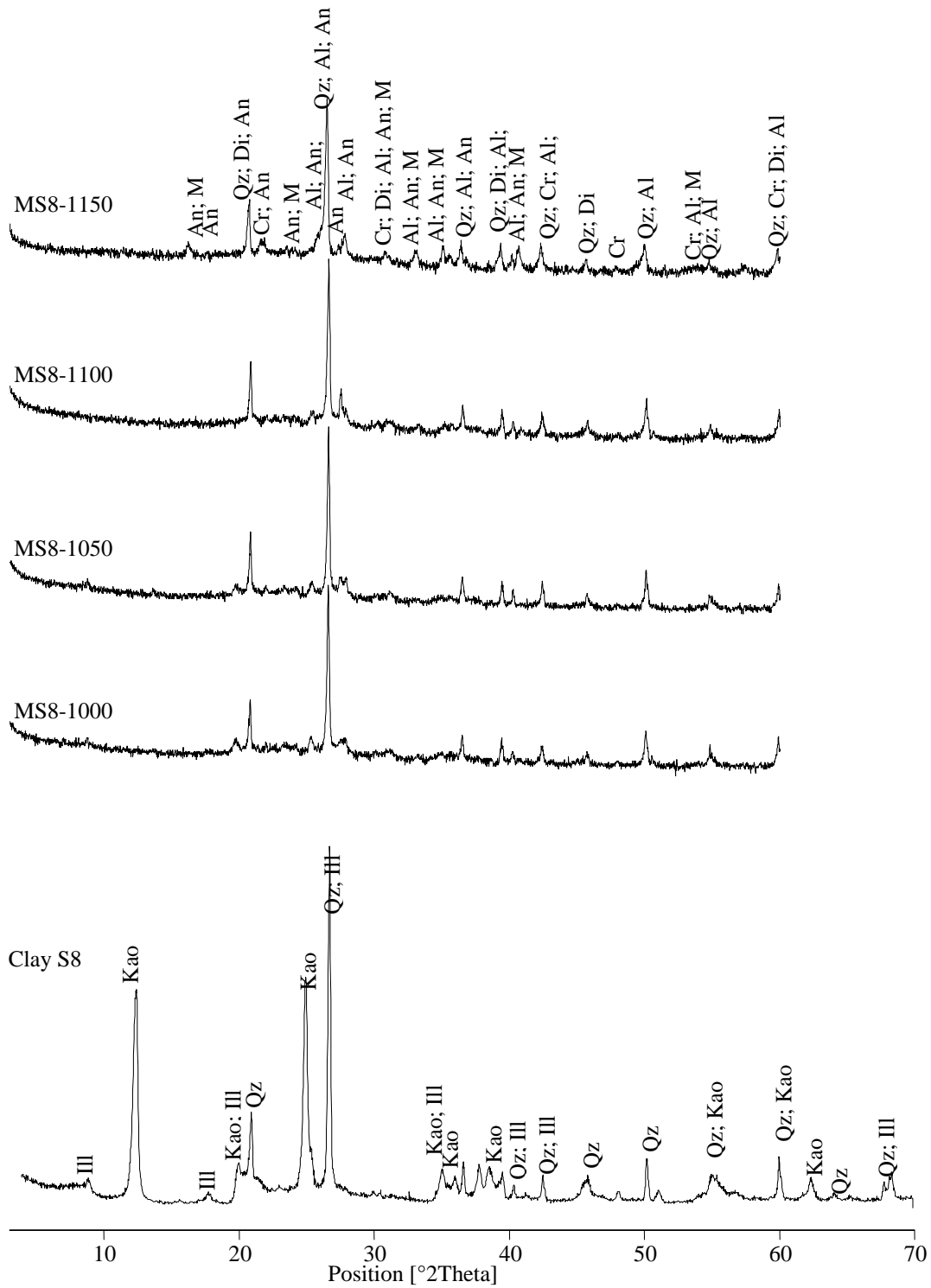
810

811

812

813

814



816

817 Fig.9: XRD patterns of S8 clay and the ceramic tiles resulting from mixture MS8 fired

818 at various temperatures (1000°C. 1050°C. 1100°C and 1150°C); Qz: quartz; He:

819 hematite; Mu: mullite; Di: diopside; Kao: kaolinite; Ill: illite

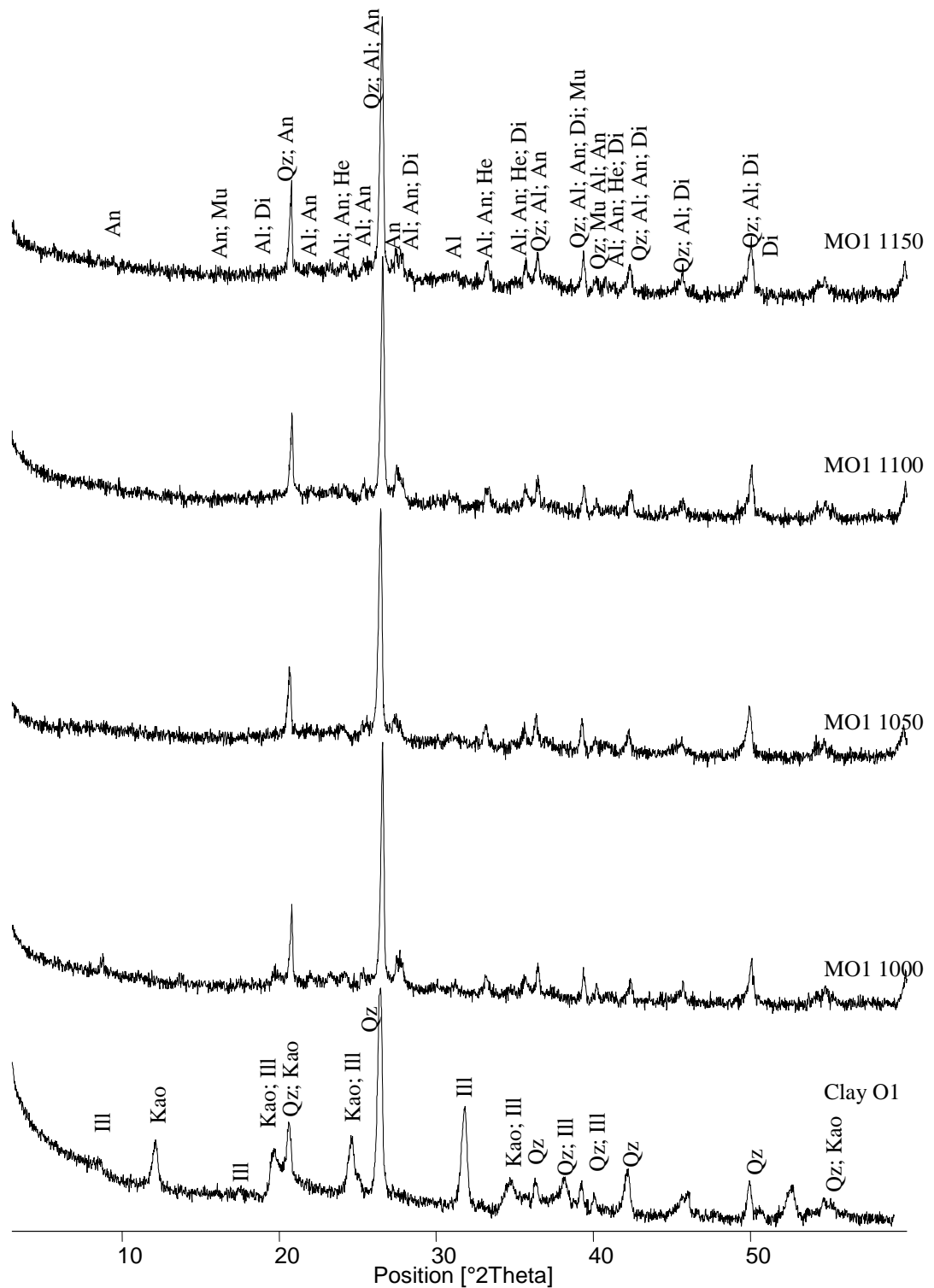
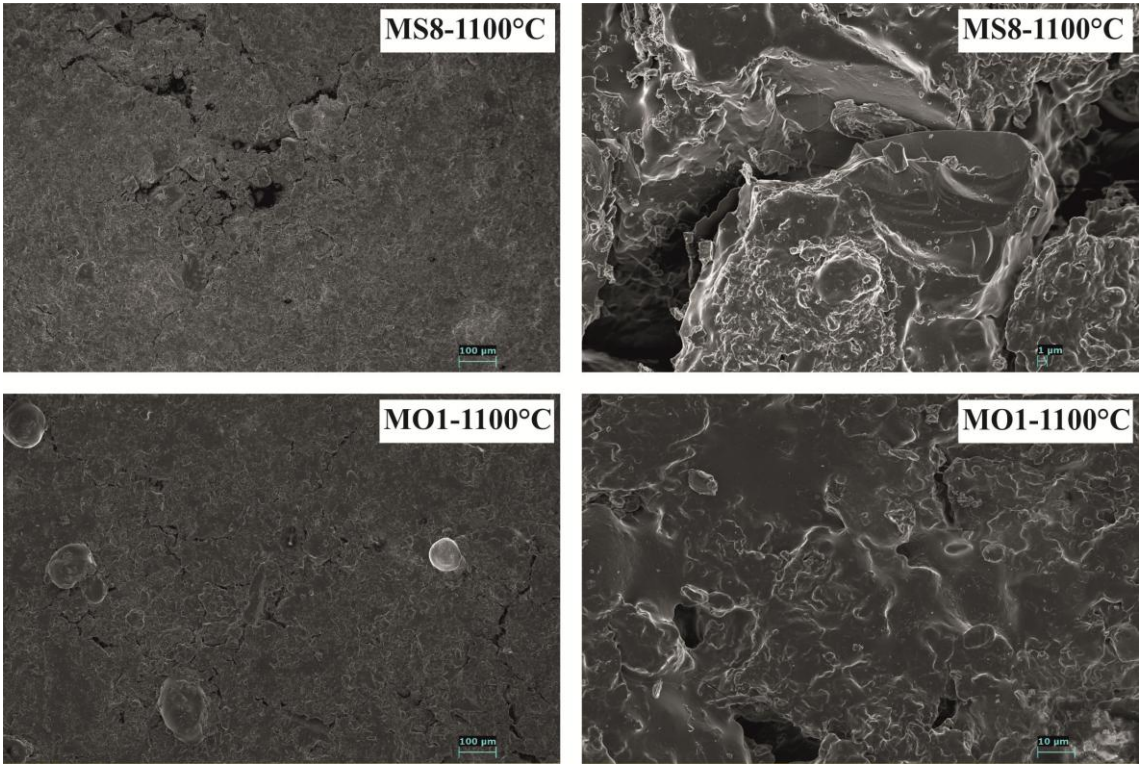


Fig. 10: XRD patterns of O1 clay and the ceramic tiles resulting from mixture MO1 fired at various temperatures (1000°C. 1050°C. 1100°C and 1150°C); Al: albite; Qz: quartz; He: hematite; Mu: mullite; Di: diopside; Kao: kaolinite; Ill: illite.

825 Fig. 11



826

827 Fig. 11: Scanning electron micrographs of tiles from mixtures MS8 and MO1.

828

829

Numidian clay deposits as raw material for ceramics tile manufacturing

B. Moussi^{1*}, W. Hajjaji², M. Hachani³, N. Hatira⁴, J.A. Labrincha⁵, J. Yans⁶ & F.

Jamoussi¹

1 Georessources Laboratory, CERTE, 273 - 8020 Soliman, Tunisia

2 Natural Water Treatment Laboratory, CERTE, 273 - 8020 Soliman, Tunisia

*3 University of Carthage Higher Institute of Environmental Science and Technology of
Borj Cedria, B.P. n° 1003 2050 Hammam Lif, Tunisia*

*4 National Office of Mines 24, Street of Energy, 2035 - Charguia – Tunis, BP: 215-
10801 Tunis Cedex – Tunisia*

*5 Materials and Ceramic Engineering Dept & CICECO. University of Aveiro. 3810-193
Aveiro. Portugal*

*6 Department of Geology, University of Namur, ILEE, Institute of Life, Earth and
Environment - 61, rue de Bruxelles, B-5000 Namur, Belgium*

* Author to whom correspondence should be addressed; phone: +216 58 795 598; fax: +216

79 325 802; email: bechirmoussi2007@gmail.com

Abstract

We investigate the potential use in traditional ceramics of several clays collected in the Numidian Flysch Formation (Upper Oligocene) at Tabarka, and Sejnane; Northern part of Tunisia). The valorization of these adopts the technique of dry process, which requires a mixture of powdered clay with 7% water. This allows rapid drying of uncooked tiles. The tiles are fired at four different temperatures (1000°C, 1050°C, 1100°C and 1150°C) in order to optimize technological parameters such as shrinkage, water absorption and flexural strength. The obtained tiles show acceptable drying and firing shrinkage (not exceeding 3%), and bending strength (between 13 and 16 N/mm²) which are close to the required standards (EN ISO 10545-4, 15N/mm² for wall tiles). The absorption ranges from 10 to 20%, which classifies these products in group BIII according to the international standards (ISO 13006 and EN ISO 10545-3). Variation of shrinkage and water absorption with the firing temperature reveals that optimal range is 1125-1150°C for the Tabarka samples, whereas the Sejnane products might be fired at lower values (~ 1025°C). The Tabarka fired pieces exhibit strong brightness. These results suggest that these latter clays could be used for white products such as sanitary ware formulations while those from Sejnane ones are more appropriated for colored (red) applications. The X-ray diffraction on the fired tiles powders shows the formation of quartz which is initially present in the crude clays, and mullite that is present at all firing temperatures. Moreover, the presence of mullite due to the richness of Al₂O₃ in Tabarka clays could support their refractory properties.

Keywords: Clays, Tabarka, Sejnane; Ceramic tiles; Technological parameters, Tunisia.

1. Introduction

The Numidian Flysch is a widespread Formation of the Tell chain located in the Northern part of Tunisia. It contains successions of clayey levels and consolidated sandstones. Previous works have been conducted to refine the geological knowledge of the Numidian Flysch (e.g., Rouvier, 1977; Fildes et al., 2009; Yaich et al., 2000; Bouaziz et al., 2002; Talbi et al., 2008; Riahi et al., 2010). Other studies have documented Pb-Zn mineralizations associated with the Numidian Clays, structurally controlled by hydrothermalism (e.g. Decree et al., 2008; Abidi et al., 2010; Jemmali et al., 2011, 2013). Felhi et al. (2008) characterized the Numidian kaolinitic clays of Tabarka.

Although Tunisia is a small country (163,610 km²), the production of ceramic tiles is developing steadily (26 million m² in 2007, growing by 12% in the last five years), due to the increasing demands of national building programs and challenges created by new opening markets (Moussi et al., 2011). There are approximately 94 Tunisian factories specialized in ceramic manufacturing, consuming about 420.000 tons in 2011 (Jeridi et al., 2014) and the development of the construction sector. Constant efforts of the economic development offices are focused on exploration for new deposits to support the increasing consumption needs, and the widespread ceramic production sites (Medhioub et al., 2012).

In this perspective, and for the purpose of researching clay deposits for ceramics, several research studies on Tunisian clay materials have been carried out (Baccour et al., (2009); Khemakhem et al., (2009). Hajjaji et al., (2010); Medhioub et al., (2010). Hachani et al., (2012); Hedfi et al., (2014, 2016); Ben M'barek Jemaï et al., (2015); Hammami-Ben Zaïed et al., (2015); Bennour et al., (2015, 2017); Ben Salah et al.,

(2016, 2018); Boussen et al., (2016); Mahmoudi et al., (2016, 2017); Zouaoui et al., (2017); Chihi et al., (2019); Kamoun et al., (2019)).

The aim of this article is to use the Numidian clays from the Tabarka and Sejnane region, which are developing regions in the ceramic industry, compare the products obtained and provide a database that could be used by investors.

Numidian clays from Sejnane have been studied and valorised in the field of ceramics (Bennour et al., 2015; Moussi, 2012). Bennour et al. (2015) studied the composition and firing behavior of these clays as a material for ceramics. Moussi (2012) studied the suitability of the Numidian clays of Cap Serrat, Gamgoum, Om Tebal and Aouinet to be used in ceramic tiles. He proved that these clays can provide important potential raw material for the manufacture of ceramic tiles. Industrially these clays are very little used in the manufacture of ceramic tiles because of their distance from the factories, which are dense in the Tunisian coastal region and Cap Bon. Some small deposits in the northwest of Tunisia were exploited for artisanal pottery.

2. Geological setting

Clays collected for this study belong to the Numidian Flysch Formation, Oligocene-Miocene in age (Rouvier, 1977; Felhi et al., 2008; Riahi et al., 2010). The Numidian Flysch results from the infilling of a peri-Mediterranean basin created between the two main tectonic events related to the Alpine Maghrebide belt (e.g. Guerrera et al., 1993 and references therein; Frizon de Lamotte et al., 2000). The first event was linked to the subduction of the Tethyan oceanic strip that separated Gondwana and the Alcapecac acronym from “Alboran basin” and the main internal massifs, from west to east

Kabylian massifs in Algeria, Peloritain Mountains in Sicily and Calabria (see Guerrera et al., 1993). The second is known as the Alpine phase and was formed by collision between the dismembered Alkapecca region and Africa. The West Mediterranean oceanic basin was created between these two main events, with an initial rifting stage (30-21 Ma, i.e., late Oligocene-Aquitania) followed by a drifting stage with the Sardinia's counterclockwise rotation during Burdigalian-Serravalian (Jolivet et Faccenna, 2000).

The sediments were deposited in a large complex of turbidite channels to fill high sediment density observed over tens of kilometers (Yaich et al., 2000). This series can locally reach ~3000 m thick and consists of three lithological units (Rouvier 1977, 1994). The series of Zouza is the lower unit; Late Oligocene in age, and has a thickness of ~1000 m in the Nefza region. It consists of a succession of sandstone lenses, clays locally oxidized, and quite rare conglomeratic horizons. The middle unit is Kroumirie sandstones, Late Oligocene in age. This latter is composed of layers of sandstone, clay and conglomerates with pebbles of quartz. The upper unit or series Babouch, Early Miocene in age, consists of gray clays. Based on planktonic foraminifera biozones, Yaich et al. (2000) date the Numidian Formation in an interval comprised between Early Rupelian and Early Burdigalian. Riahi et al. (2010) present a new dating (Oligocene to early Miocene) for the two first units, based on new biostratigraphic data from the analysis of planktonic foraminifera. Yaich et al. (2000), mean while, proposed the establishment of the Numidian between Langhian and Serravallian (13 Ma), corresponding to the intrusion of endogenous igneous rocks in the area (see Decrée et al., 2014).

The origin of the sediments forming the Numidian was widely debated. The provenance from the North is based on the presence of current ripples in Numidian formations (Wildi, 1983; Parize et al., 1986; Talbi, 1998). This hypothesis is consistent with recent studies that suggest a European Nordic sediment provenance, based on the study of zircons (Fildes et al., 2009). Alternatively, Wezel (1970), based on the morphology of quartz grains, proposes a Southern source of Numidian, from the Nubian Sandstone. Accordingly, the analysis of sedimentary structures by Hoyez (1975) suggests that the Numidian is located at the edge of Saharian zone. This hypothesis was recently overturned by Yaich et al. (2000), based on biostratigraphic arguments. Anyway, the origin of the kaolinitic-illitic clays would be related to the weathering/alteration of the feldspars of the Numidian Flysch (Crampon, 1973). The area experienced complex phases of weathering and alteration, leading to the neoformation of halloysite/kaolinite in several rocks (Decree et al., 2008; Sghaier et al., 2014). The lithological succession (Fig. 1 and 2) of the two studied sites provides a good estimate of the reserves of kaolinitic-illitic clays in the area.

3. Materials and methods

Two sites were studied: Sidi El Bader close to Tabarka city and Om Tebal close to Sejnane city (Fig.1). Sidi El Bader area is located east of the town of Tabarka limited by the Jebel Touila at its east side. Four representative samples (50 kg each) were collected: S8 and S9 from Tabarka, O1 and O4 from Sejnane.

Mineralogical analyses of bulk samples were carried out by X-ray diffraction (XRD), using an X-ray Panalytical X'Pert Pro diffractometer (Cu-K α radiation (1,540598Å), 2 θ range from 3° to 60°). The relative amounts of phases were estimated by measuring the

areas of the main peaks (Torres- Ruiz et al., 1994; López-Galindo et al., 1996) using the Panalytical X'Pert HighScore Plus software. Oriented aggregates were treated with ethylene glycol and heated at 550°C for 2 h. The chemical composition of powdered samples was determined by X-ray fluorescence; with a Panalytical Axios Dispersive XRF Spectrometer using the conventional techniques (Meseguer et al., 2009). The loss-on-ignition was evaluated from the weight difference between samples heated at 100°C and 1000°C. The results are expressed in concentration percent of oxides. The Casagrande method was selected for the determination of the Atterberg limits (LCPC, 1987; Grabowska-Olszewska, 2003) with an experimental error of $\pm 3\%$. The grain-size distribution of as-received samples was obtained by wet sieving, using an AFNOR series device adopted by the French standardization system. The fraction $< 63 \mu\text{m}$ was completed by laser diffraction using Mastersizer 2000 granulometer. Thermal analyses TDA-TGA were performed using Netzsch STA409/429 equipment with a heating rate of 10 K min^{-1} and by using $\alpha\text{-Al}_2\text{O}_3$ as the inert marker. Dilatometric analysis was conducted on a Netzsch 402E dilatometer at a maximum temperature of 1000°C (5°C min^{-1} heating rate). The thermal behavior was studied by DTA-TG analyses (Setaram apparatus) in air atmosphere with $10^\circ\text{C min}^{-1}$ heating rate. The Bigot curves were obtained under room-temperature conditions by using an Adamel barelattograph. The clayey material was crushed and rolled for a coarse grain size of 1mm. The shaping of the clay requires certain amount of water into pieces of dimension 15x15x30mm (to measure the weight and length of wet pieces). These pieces were subjected to drying in open air conditions in the apparatus of Adamel Barellatograph. This device can track and trace drying curve according to the mass loss. At the end of drying, the pieces were weighed and oven dried for 24 hours at 110°C for measuring the final mass and dry

lengths. These parameters allow at measuring the drying shrinkage and water required for shaping, interposition and colloidal.

The ceramics tiles were shaped by dry pressing and the material was dried and crushed before sieving. The moisture level was adjusted to 6-7 wt% and the powders were pressed (250 bars) into 50x50x100 mm pieces (Moussi et al., 2011). These tiles were dried overnight at 40°C + 8h at 110°C. Then the samples were fired at maximum temperatures of 1000, 1050, 1100 and 1150°C (15°C/min, heating rate and 30 min dwell time), approaching industrial conditions (Jeridi et al., 2008). Shrinkage on drying and firing was determined manually. The bending strength of the fired bodies was determined on a LCV F006 NANETTI Fleximeter and the water absorption was assessed following European standards (UNI EN ISO 10545-3). Phases formed after firing were characterized by XRD while the microstructure was studied by scanning electron microscopy (SEM, Hitachi SU70, Bruker AXS detector, Quantax software). To improve the quality of ceramic products obtained with crude clays, separate mixtures were prepared by combining Tabarka and Sejnane clays with silica sand, carbonated clay (RGS) and feldspars (Table 2). These mixtures have undergone the same processes as shaping, drying and firing as previously described with ceramic tiles without additions.

Carbonated clay was added to the mixtures due to the richness of calcium carbonate (14%). An addition of carbonate is therefore desired in order to create a porosity. In fact, these carbonates are considered to be fluxes, extending glassy phases (Kazmi et al., 2017). Feldspars have been added for the same reason as a fluxing agent. Silica sand has been added to enhance the hardening qualities and increase the flexural strength.

RGS carbonate clay is collected in the Nefza region, between Tabarka and Sejnane. It is a clay of Lutetian-Bartonian age locally qualified "argile noire à boules Jaune" with dolomitic concretions. These clays belong to the tellian facies (Rouvier, 1977). The added sand belongs to the Beglia formation of lower Miocene age harvested from the Saouaf region.

4. Results and discussion

The X- ray diffraction patterns (Table 1) show a kaolinitic-illitic content of the samples collected from both studied sites. Mixed-layers I-S were also identified in O1 sample. Moreover, an important quartz fraction (superior to 25%) is detected and directly influences the rheological behavior of clays. The Holtz & Kovacs (Fig. 3) classified these clays as moderate plastic, with the exception of O4 which is considered highly plastic. The large amount of clay minerals (75%) can explain this plasticity behavior of this last sample. Hajjaji et al. (2010) have shown that when the quantity of phyllosilicates increases, the limits of Atterberg also increase. This plastic behavior of the samples is closely related to the presence of coarse grains of silts and sands as well as the mineralogical composition. Although these clays are placed above the domain of kaolinite and illite in the diagram of Holtz & Kovacs these clays are rich in kaolinite this is explained by the richness in grain of sand which decrease the index of plasticity.

This variation could lead to the appearance of cracks after drying process (Jordan et al., 1999). These results are comparable to the mineralogical study by Bennour et al., (2015). they prove the existence of kaolinite, illite and I/S mixed-layers associated with quartz. As for the study by Hammami-Ben Zaied et al., (2015), these authors studied Miocene Gram clays. They proved an excessive richness of these clays in quartz but

despite these results they proved the aptitude for the use of these excessively degreaser clays for the manufacture of Ceramic bricks with mixtures.

The silica contents (SiO_2) are within the desirable range as ceramic raw material, not exceeding 60wt.% (Tab.1). The concentrations of alkaline oxides (Na_2O and K_2O) are relatively low and consistent with the contents of illite and absence of fluxing agents such as feldspars. The iron oxides and hydroxides contents in the Tabarka clays are very low (0.01 to 1.14 wt. %) in comparison to Sejnane clays (5.5 to 7.6 wt. % of Fe_2O_3). This could generate white ceramic product. The total loss on ignition is relatively high in the Tabarka samples (10.78%) compared to the Sejnane samples (9.77%). This loss on ignition is dependent on the decomposition of clay minerals (kaolinite), the removal of absorbed and crystalline water and the alkali content. The high loss on ignition detected in RGS carbonate clay is 14.35%, it is due to the decomposition of kaolinite and carbonates.

The particle size distribution curves of the clays studied show similar shapes for both Tabarka and Sejnane clays. According to the particle size distribution curves, the fraction less than 2 μm is large about 63 -70% for S8 and S9 while O1 and O4 are on the order of 53 to 63%. The high fraction contents below 2 μm is closely related to the mineralogical composition rich in kaolinite. The coarse silty and sandy fractions are then important. These results are in perfect correlation with the mineralogy of clays. The study of these particle size curves as well as the Bigot curves reveal the quantities of sand to be added to the mixture used for the manufacture of ceramic tiles. The particle size distribution curve of the added sand shows a coarse fraction not exceeding 300 μm . its medium sized sand fig. 4).

The drying behavior can be deduced from the Bigot curves (Fig. 5). These clays have a relatively high drying shrinkage (around 5%) consistent with the plasticity values. The drying behavior is a parameter used in the ceramic industry as the prime indicator for selection of the raw material (Dondi et al., 1998, Meseguer, 2010). This behavior is deduced from the Bigot curves. According to the curves, we notice a total mass loss of 20.8% for the Tabarka clays and 25.5% for the Sejnane clays. This loss of mass is characterized by two stages. The first mass loss consists of the colloidal water loss which is 14.61% for the Tabarka clays and 10.07% for that of Sejnane. This proves that the latter are characterized by a faster drying than Tabarka clays. The second loss of mass is linked to the departure of the interposition water which are 6.19% and 15.45% respectively for S9 and O1. According to these results, Tabarka clays have a slow drying behavior which suggests the addition of a degreaser.

According to the particle size distribution curves, Tabarka clays are finer than Sejnane clays and therefore require a significant amount (15%) of sand as a degreaser. However only 5% of sand has been added to Sejnane clays and this is to avoid faults during drying and firing and to ensure good resistance to bending. The thermal behavior of these Numidian clays is reported in Figure 6. The water of hydration in the interlayer space disappeared at a temperature between 60 and 100°C. An endothermic peak on the DTA curve appears around the same temperatures. At 550°C, the expulsion of constitution water dehydroxylation is depicted by a second major endothermic peak. At this stage, the mass loss is between 8 and 10%, which is in accordance with the LOI (Table 1).

Formulations of the ceramic tiles are reported in Table 2. The Tabarka samples S8 and S9 show the similar expansion behavior with a total shrinkage of 0.66% and 1.05% for S8 and S9, respectively (Table 3, Fig. 7). A higher shrinkage is recorded on the Sejnane

samples due to the richness in melting (sum Fe_2O_3 , MgO , CaO , Na_2O and K_2O equal to 11%) compared to Tabarka clays (4%). These fluxes tend to promote vitrification and increase shrinkage (Tite et Maniatis, 1975, in Cultrone et al., 2001).

Concerning the bending strength, the values increase with temperature but do not exceed 5.3MPa (table 3) and are below the required standards of ceramic wall tiles (ISO 10545-4, 2004). As a consequence, various corrections in compositional mixtures were implemented to improve the mechanical strength, as discussed below.

The values of the drying shrinkage are of the order of 1.11% and 0.21% for ceramic tiles obtained from S8 and S9, respectively, and 1.55 and 1.47 for O1 and O4. These values are relatively high and should be minimized using the silica sand addition. The water absorption classifies these products in the BIII group of international standards (ISO 13006) with the exception of products O1 and O4 fired at 1150°C that belong to the BII group.

Compared to previous compositions (made exclusively of crude clays), the mixture products inhibited lower drying shrinkages close to 0.5 % (Table3). The firing shrinkage is lower than 2.5%. A good pressure (250- 280bars) applied to the tiles at a 6-7% humidity rate helped to avoid the lamination problems (Padoa, 1982). The bending strengths range from 13 to 16 N/mm^2 and are considered as close to the international standards for wall tiles requirements (15MPa) (Table3). This criterion reflects a good densification of the ceramics tiles. In comparison with the values of parameters of the crude products (Table 3), the results of the various parameters of the ceramics tiles resulting from the mixtures show a significant improvement. The water absorptions, ranging from 10.98% to 14.48% (Fig.8), classify these products as group BIII (ISO 13006- and NF EN ISO 10545-3). The Figure 9 shows the relationship between water

absorption and firing shrinkage. The intersection of both curves allows at choosing the optimum temperatures for firing these products in order to minimize the processing costs. According to these observations, it obvious that the Tabarka products require higher firing temperatures (1120 to 1150°C). These temperatures are close to the sanitary ware ceramic firing temperatures, and consequently these clays can constitute a good raw material for these applications. For Sejnane based products, the firing temperature should be lower (about 1020°C). These ceramic tiles are dark red colored and present a good quality aspect.

The firing transformations are represented by X-ray diffraction in figures 9 and 10. The X-ray diffractions of the raw mixtures before firing are compared with those fired at 1000, 1050, 1100 and 1150 °C. The crude mixtures show the richness in Kaolinite and in illite in the presence of quartz. According to DTA, the kaolinite disappears at 550°C, on the other hand from 1000°C (both case of MO1 1000 and S8 1000) the amount of illite decreases to disappear at 1050 ° C. From 1100 ° C, the beginning of the formation of mullite is recorded (reference code: 2-431) marked by the peak at 5.39Å. Mullite is an important ceramic material because of its low density, high thermal stability, and stability in severe chemical environments (Cao et al., 2004). For a higher temperature (1150 °C), a peak at 4.06Å only for fired products of Tabarka records the formation of cristobalite (reference code 1-76-939). A peak at 2.94Å appears on the X-rays diffractograms of the all fired product of Tabarka and Sejnane attributed to the formation of the diopside (reference code 1-83-1820). The Sejnane clays are rich in iron oxide (Table 1). These iron oxides contributed to the formation of hematite (Fig.10) recorded only on fired products of Sejnane and marqued by a peak at 2.69Å (code reference 1-1053) which ensures a certain rigidity of the ceramics tiles (high bending strength), due to its fluxing character. The quartz initially present in the mixtures of raw

clays persists during all firing phases. The presence of silicon, alkaline and calco-alkali compounds support the formation of plagioclases (albite and anorthite) (Lee et al., 2008) which appear from 1000 ° C but their quantities increase depending on the temperature.

Few pores are visible on the SEM observations (Fig.11). At the temperature of 1050°C and 1100°C, these materials show the same crystalline structure with the presence of siliceous glass. The SEM observation of ceramic tiles MO1 reveal the presence of significant amount of glassy phase. The quartz occupies the voids between the particles.

These products can be judged of good quality because of their good technological characteristics and appearance. There are no major defects detected during drying and firing. Defects revealed upon the use of raw clay were corrected by the addition of sand and feldspar. The addition of carbonated clay reduced the firing temperatures. Carbonated clay (RGS) was added (20%) in all mixtures with the aim of increasing the CaO content and promoting the formation of a glassy phase (Kazmi et al., 2017) because these crude clays have a low CaO content (table 1). Moreover, the presence of calcite, dolomite or both can influence the formation of different minerals at high temperatures (Trindade et al., 2010). The presence of fluxing oxides including Fe₂O₃ tend to reduce the temperature at which a partial melt is formed (Abdelmalek et al., 2017). The iron oxide is the main colorant in clayey materials, responsible for the reddish color observed after firing (Abajo, 2000 in Abdelmalek et al., 2017).

These materials can be considered as refractory because of its high content in kaolinite and sand (Hachani et al., 2012). Therefore, these Oligocene clays of northern Tunisia can be a good raw material for the manufacture of ceramic tiles. The clays of Tabarka can be used in the production of sanitary ceramics due to their fine clay particles and

their good densification during firing at high temperatures. These trials made in the laboratory must be supplemented with other mixtures of clays and on an industrial scale to confirm their ability to be a good raw material for ceramics.

Conclusion

The Tabarka and Sejnane clays, which belong to the Numidian Flysch, whose thicknesses can reach 3000 meters, were studied in order to decipher their use in ceramic manufacturing. The characterization of the raw clays shows a mineralogy composition dominated by kaolinite and illite and relatively high quartz content for the two sites of Tabarka and Sejnane. Chemical analyzes show a significant richness in SiO_2 ; this can be explained by the presence of clays and silica sand. The mineralogical and chemical results are consistent. According to the particle size distribution curves, the Sejnane clays have a larger coarse particle size fraction compared to those of Tabarka which influences the percentage of sand additions as degreaser. These clays were tested in the manufacture of ceramic tiles. Technological tests show the aptitude of these raw materials to be used in the manufacture of ceramic tiles on an industrial scale. The aspect of ceramic tiles is acceptable with characteristics close to the required standards. In particular, the drying and firing shrinkages are low, the flexural strength and the water absorption are also within the standard limits. Tabarka ceramic tiles have a white color due to the richness in kaolinite and the rarity of iron oxides. These clays can be used as raw materials for ceramic tiles. Sejnane ceramic tiles have a red color due to the richness of iron oxide initially present in raw clays. These very abundant Numidian clays alternate in succession with metric, sometimes decametric, levels of consolidated sandstone. These geological outcrops extended to the northwest of Tunisia

in the Tellian domain, present immense geological deposits of industrially useful raw material.

Acknowledgment

This research was financed by the Ministry of Higher Education, Scientific Research and Technology (Tunisia), and the Belgian-Tunisian project “Valorisation des argiles” of the Wallonie-Bruxelles International (WBI). Thanks are due for the support of the CTMCCV (Centre Techniques de Matériaux de Construction de Céramique et du Verre Tunis - Tunisie).

References

- Abajo, M.F., 2000. Manual sobre fabricación de baldosas, tejas y ladrillos. Ed. Beralmar S. A., (Barcelona).
- Abdelmalek, B., Rehia, B., Youcef, B., Lakhdar, B., Nathalie, F., (2017). Mineralogical characterization of Neogene clay areas from the Jijel basin for ceramic purposes (NE Algeria -Africa). *Applied Clay Science*, 136, 176–183. doi:10.1016/j.clay.2016.11.025.
- Abidi R., Slim-Shimi N., Somarin A., Henchiri M., (2010). Mineralogy and fluid inclusions study of carbonate-hosted Mississippi valley-type Ain AllegaPb–Zn–Sr–Ba ore deposit, Northern Tunisia. *Journal of African Earth Sciences* 57, (2010) 262–272. <https://doi.org/10.1016/j.jafrearsci.2009.08.006>
- Baccour H., Medhioub M., Jamoussi F., & Mhiri T. (2009). Influence of firing temperature on the ceramic properties of Triassic clays from Tunisia. *Journal of Materials Processing Technology*, 209(6), 2812–2817. doi:10.1016/j.jmatprotec.2008.06.055
- Ben M’barek Jemaï M., Sdiri A., Errais E., Duplay J., Ben Saleh I., Zagarni M. F., & Bouaziz S. (2015). Characterization of the Ain Khemouda halloysite (western Tunisia) for ceramic industry. *Journal of African Earth Sciences*, 111, 194–201. doi:10.1016/j.jafrearsci.2015.07.014
- Ben Salah I., M’barek Jemaï M. B., Sdiri A., Boughdiri M., & Karoui N. (2016). Chemical and technological characterization and beneficiation of Jezza sand (North West of Tunisia): Potentialities of use in industrial fields. *International Journal of Mineral Processing*, 148, 128–136. doi:10.1016/j.minpro.2016.01.016

411 Ben Salah I., Sdiri A., Ben M'barek Jemai M., & Boughdiri M. (2018). Potential use of
 412 the lower cretaceous clay (Kef area, Northwestern Tunisia) as raw material to
 413 supply ceramic industry. *Applied Clay Science*, 161, 151–162.
 414 doi:10.1016/j.clay.2018.04.015

415 Bennour A., Mahmoudi S., & Srasra E. (2017). Physico-chemical and geotechnical
 416 characterization of Bargou clays (Northwestern Tunisia): application on traditional
 417 ceramics. *Journal of the Australian Ceramic Society*, 54(1), 149–159.
 418 doi:10.1007/s41779-017-0136-5

419 Bennour A., Mahmoudi S., Srasra E., Boussen S., & Htira N. (2015). Composition,
 420 firing behavior and ceramic properties of the Sejnène clays (Northwest Tunisia).
 421 *Applied Clay Science*, 115, 30–38. <https://doi.org/10.1016/j.clay.2015.07.025>

422 Bouaziz S., Barrier E., Soussi M., Turki M. M., Zouari H., (2002). Tectonic evolution
 423 of the northern African margin in Tunisia from paleostress data and sedimentary
 424 record. *Tectonophysics*, 357, (2002) 227-253. [https://doi.org/10.1016/S0040-](https://doi.org/10.1016/S0040-1951(02)00370-0)
 425 [1951\(02\)00370-0](https://doi.org/10.1016/S0040-1951(02)00370-0)

426 Boussen S., Sghaier D., Chaabani F., Jamoussi B., & Bennour A. (2016).
 427 Characteristics and industrial application of the Lower Cretaceous clay deposits
 428 (Bouhedma Formation), Southeast Tunisia: Potential use for the manufacturing of
 429 ceramic tiles and bricks. *Applied Clay Science*, 123, 210–221.
 430 doi:10.1016/j.clay.2016.01.027

431 Cao X. Q., Vassen R., Stoeber D., (2004). Ceramic materials for thermal barrier
 432 coatings. *Journal of the European Ceramic Society* 24, (2004) 1–10.
 433 [https://doi.org/10.1016/S0955-2219\(03\)00129-8](https://doi.org/10.1016/S0955-2219(03)00129-8)

434 Chihi R., Blidi I., Trabelsi-Ayadi M., & Ayari F. (2019). Elaboration and
 435 characterization of a low-cost porous ceramic support from natural Tunisian
 436 bentonite clay. *Comptes Rendus Chimie*. doi:10.1016/j.crci.2018.12.002

437 Crampon N., (1973). L'extrême nord tunisien. Aperçu stratigraphique, pétrologie et
 438 structural. Livre jubilaire M. Solignac. *Ann. Min. et Géol. Tunis.*; 26, pp. 49–85.

439 Decrée S., De Putter T., Yans J., Moussi B., Recourt P., Jamoussi F., Bruyère D. &
 440 Dupuis C., (2008). Iron mineralization in marginal basins surrounding Fe-Pb-Zn
 441 sulphide deposits (Neogene Tunisian Tell, Nefza district): mixed influence of
 442 pedogenesis and hydrothermal alteration. *Ore Geology Reviews* 33, 3-4, 397-410.
 443 <https://doi.org/10.1016/j.clay.2018.07.007>

444 Decrée S., Marignac C., Liégeois J. P., De Putter T., Yans J., Ben Abdallah R.,
 445 Demaiffe D., (2014). Miocene magmatic evolution in the Nefza District (Northern
 446 Tunisia). *Lithos* 192-195, 240-258. <https://doi.org/10.1016/j.lithos.2014.02.001>

447 Dondi, M., Marsigli, M., Ventura, I., 1998. Sensibilità all'esiccamento e caratteristiche
 448 porosimetriche delle argille italiane per laterizi. *Ceramurgia* 28, 1–8.

449 Felhi M., Tlili A., Gaied M. E., Montacer M., (2008). Mineralogical study of kaolinitic
 450 clays from Sidi El Bader in the far north of Tunisia. *Applied Clay Science* 39 p208–
 451 217.

452 Fildes C., Stow D.A.V., Riahi S., Soussi M., Patel U., Milton J.A., Marsh S., (2009).
 453 European Provenance of the Numidian Flysch in northern Tunisia. *Terra Nova*, Vol
 454 22, No. 2, 94–102. <https://doi.org/10.1111/j.1365-3121.2009.00921.x>

455 Frizon de Lamotte D., Saint-Bezar B., Bracene R., Mercier E., (2000). The two main
 456 steps of the Atlas building and geodynamics of the western Mediterranean.
 457 Tectonics, 19, 740–761. <https://doi.org/10.1029/2000TC900003>

458 Grabowska-Olszewska B., (2003). Modelling physical properties of mixtures of clays:
 459 example of two component mixture of kaolinite and montmorillonite. Applied Clay
 460 Science, 22, 251-259. [https://doi.org/10.1016/S0169-1317\(03\)00078-4](https://doi.org/10.1016/S0169-1317(03)00078-4)

461 Guerrera F., Martin-Algarra A., Perrone V., (1993). Late Oligocene-Miocene syn-late-
 462 orogenic successions in western and central Mediterranean chains from the Betic
 463 Cordillera to the Southern Apennines: Terra, Nova, 5, 525–544.
 464 <https://doi.org/10.1111/j.1365-3121.1993.tb00302.x>

465 Hachani M., Hajjaji W., Moussi B., Medhioub M., Rocha F., Labrincha J. A., &
 466 Jamoussi F. (2012). Production of ceramic bodies from Tunisian Cretaceous clays.
 467 Clay Minerals, 47(01), 59–68. doi:10.1180/claymin.2012.047.1.59

468 Hajjaji W., Moussi B., Hachani M., Medhioub M., Lopez-Galindo A., Rocha F.,
 469 Jamoussi F. (2010). The potential use of Tithonian–Barremian detrital deposits from
 470 central Tunisia as raw materials for ceramic tiles and pigments. Applied Clay
 471 Science, 48(4), 552–560. doi:10.1016/j.clay.2010.03.003

472 Hammami-Ben Zaied F., Abidi R., Slim-Shimi N., & Somarin A. K. (2015). Potentiality
 473 of clay raw materials from Gram area (Northern Tunisia) in the ceramic industry.
 474 Applied Clay Science, 112-113, 1–9. doi:10.1016/j.clay.2015.03.027

475 Hedfi I., Hamdi N., Rodriguez M. A., & Srasra E. (2016). Development of a low cost
 476 micro-porous ceramic membrane from kaolin and Alumina, using the lignite as

477 porogen agent. Ceramics International, 42(4), 5089–5093.
478 doi:10.1016/j.ceramint.2015.12.023

479 Hedfi I., Hamdi N., Srasra E., & Rodríguez M. A. (2014). The preparation of micro-
480 porous membrane from a Tunisian kaolin. *Applied Clay Science*, 101, 574–578.
481 doi:10.1016/j.clay.2014.09.021

482 Holtz, R.D., Kovacs, W.D., 1981. *An Introduction to Geotechnical Engineering*.
483 Prentice-Hall, Englewood Cliffs, New Jersey.

484 Hoyez, B., (1975). Dispersion du matériel quartzeux dans les formations aquitaniennes
485 de Tunisie septentrionale et d’Algérie nord-orientale. *Bull. Soc. Géol. Fr.*, XVII :
486 1147-1156.

487 ISO 10545-3, (1995). *Ceramic tiles. Part 3: Determination of water absorption, apparent*
488 porosity, apparent relative density and bulk density. Edition 1.

489 ISO 10545-4, (2004). *Ceramic tiles. Part 4: Determination of modulus of rupture and*
490 breaking strength. Edition 2.

491 ISO 13006, (2012). *Carreaux et dalles céramiques — Définitions, classification,*
492 caractéristiques et marquage.

493 Jemmali N., Souissi F., Carranza E. J. M., Vennemann T. W., (2013). Mineralogical and
494 Geochemical Constraints on the Genesis of the Carbonate-Hosted Jebel Ghazlane
495 Pb-Zn Deposit (Nappe Zone, Northern Tunisia). *Resource Geology* Volume 63,
496 Issue 1, January 2013, Pages 27-41. doi: 10.1111/j.1751-3928.2012.00208.x

497 Jemmali N., SouissiF., Villa I. M., Vennemann T. W., (2011). Ore genesis of Pb-Zn
498 deposits in the Nappe zone of Northern Tunisia: Constraints from Pb-S-C-O isotopic

499 systems. *Ore Geology Reviews* Volume 40, Issue 1, September 2011, Pages 41-53.
500 doi.org/10.1016/j.oregeorev.2011.04.005

501 Jeridi K., Hachani M., Hajjaji W., Moussi B., Medhioub M., Lopez-Galindo A., Kooli
502 F., Zargouni F., Labrincha J.A. & Jamoussi F., (2008). Technological behaviour of
503 some Tunisian clays prepared by dry ceramic processing. *Clay Minerals*, 43, 339-
504 350. DOI: 10.1180/claymin.2008.043.3.01

505 Jeridi K., López-Galindo, A., Setti M., Jamoussi F., (2014). The use of Dynamic
506 Evolved Gas Analysis (DEGA) to resolve ceramic defects. *Applied Clay Science*,
507 Volume 87, January 2014, Pages 292-297.
508 <https://doi.org/10.1016/j.clay.2013.10.021>

509 Jolivet L., and Faccenna C., (2000). Mediterranean extension and the African-Eurasia
510 collision. *Tectonics*, 19, 1095–1106. <https://doi.org/10.1029/2000TC900018>

511 Jordan M. M., Boix A., Sanfeliu T., De la fuente C., (1999). Firing transformations of
512 cretaceous clays used in the manufacturing of ceramic tiles, *Appl. Clay Sci.* 14, pp.
513 225-234. [https://doi.org/10.1016/S0169-1317\(98\)00052-0](https://doi.org/10.1016/S0169-1317(98)00052-0)

514 Kamoun N., Jamoussi F., & Rodríguez M. A. (2019). The preparation of meso-porous
515 membranes from Tunisian clay. *Boletín de La Sociedad Española de Cerámica y*
516 *Vidrio*. doi:10.1016/j.bsecv.2019.06.001

517 Kazmi S.M., Abbas S., Nehdi M.L., Saleem M.A., Munir M.J., (2017). Feasibility of
518 using waste glass sludge in production of ecofriendly clay bricks. *J. Mater. Civ.*
519 *Eng.* 29, 4017056. DOI: 10.1061/(ASCE)MT.1943-5533.0001928

520 Khemakhem S., Larbot A., & Ben Amar R. (2009). New ceramic microfiltration
 521 membranes from Tunisian natural materials: Application for the cuttlefish effluents
 522 treatment. *Ceramics International*, 35(1), 55–61.
 523 doi:10.1016/j.ceramint.2007.09.117

524 LCPC, (1987). Limites d'Atterberg, limite de liquidité, limite de plasticité. Méthode
 525 d'essai n°19, Laboratoire Central des Ponts et Chaussées, 26 pp.

526 Lee W.E., Souza G.P., McConville C.J., Tarvornpanich T., Iqbal Y., (2008). Mullite
 527 formation in clays and clay-derived vitreous ceramics. *Journal of the European*
 528 *Ceramic Society* 28 - 465–471. <https://doi.org/10.1016/j.jeurceramsoc.2007.03.009>

529 López-Galindo A., Torres-Ruiz J. & Gonzalez-López J.M., (1996). Mineral
 530 quantification in sepiolite-palygorskite deposits using X-ray diffraction and
 531 chemical data. *Clay Minerals*, 31, 217-224. DOI:
 532 <https://doi.org/10.1180/claymin.1996.031.2.07>

533 Mahmoudi S., Bennour A., Srasra E., & Zargouni F. (2016). Determination and
 534 adjustment of drying parameters of Tunisian ceramic bodies. *Journal of African*
 535 *Earth Sciences*, 124, 211–215. doi:10.1016/j.jafrearsci.2016.09.031

536 Mahmoudi S., Bennour A., Srasra E., & Zargouni F. (2017). Characterization, firing
 537 behavior and ceramic application of clays from the Gabes region in South Tunisia.
 538 *Applied Clay Science*, 135, 215–225. doi:10.1016/j.clay.2016.09.023

539 Medhioub M. , Baccour H., Jamoussi F., Mhiri T. (2010). Composition and ceramic
 540 properties of triassic clays from Tunisia. *Journal of Ceramic Processing*
 541 *Research* Volume 11, Issue 2, 2010, Pages 209-214

542 Medhioub M., Hajjaji W., M. Hachani, Lopez-Galindo A., Rocha F., Labrincha J.A.
 543 &Jamoussi F. , (2012). Ceramic Tiles Based On Central Tunisian. Clays (SidiKhalif
 544 Formation), Clay Minerals, (2012) 47, 165–175. DOI: [https:// doi.org/10.1180/](https://doi.org/10.1180/claymin.2012.047.2.02)
 545 claymin. 2012.047.2.02

546 Meseguer S., Sanfeliu T., Jordan M.M. , (2009). Classification and statistical analysis of
 547 mine spoils chemical composition from Oliete Basin (Teruel. NE Spain).
 548 Environmental Geology 56, 1461–1466. DOI:10.1007/s00254-008-1241-0

549 Meseguer, S., 2010. Ceramic behaviour of five Chilean clays which can be used in the
 550 manufacture of ceramic tile bodies. Appl. Clay Sci. 47, 372–377.
 551 <https://doi.org/10.1016/j.clay.2009.11.056>

552 Moussi B., 2012. Thèse de doctorat en sciences géologique . Mode de genèse et
 553 valorisation de quelques argiles de la région de Nefza-Sejnane (Tunisie
 554 Septentrionale)., Université de Carthage, Tunisie .157p.

555 Moussi B., Medhioub M., Hatira N., Yans J., Hajjaji W., Rocha F., Labrincha J.A.
 556 &Jamoussi F. , (2011). Identification and use of white clayey deposits from the area
 557 of Tamra (Northern Tunisia) as ceramic raw materials. Clay Minerals, (2011) 46,
 558 165–175. <https://doi.org/10.1180/claymin.2011.046.1.165>

559 Padoa L., (1982). La cottura dei prodotti ceramici. Terza Edizione, Faenza Editrice,
 560 Italy. 299 pp.

561 Parize O., Beaudoin B., Burollet P.F., Cojan G., Fries G., Pinault M., (1986). La
 562 provenance du matériel gréseux numidien est septentrionale (Sicile et Tunisie). C.R.
 563 Acad. Sci. Paris, 18: 1671-1674.

564 Riahi S., Soussi M., Boukhalfa K. Ben Ismail Lattrache K, Dorrik S., Khomsi S., Bedir
 565 M., (2010). Stratigraphy, sedimentology and structure of the Numidian Flysch thrust
 566 belt in northern Tunisia. *Journal of African Earth Science* 57 (109–126).
 567 <https://doi.org/10.1016/j.jafrearsci.2009.07.016>

568 Rouvier H., (1977). *Géologie de l'extrême Nord-Tunisien: tectonique et*
 569 *paléogéographie superposées à l'extrémité orientale de la chaîne Nord-Maghrebine.*
 570 *Thèse de doctorat, Université Pierre et Marie Curie (Paris, France), 215p.*

571 Rouvier H., (1994). Notice explicative de la carte géologique de la Tunisie au 1/50000e
 572 – Nefza, feuille 10. Office National des Mines, Direction de la Géologie, 48p.

573 Sghaier D., Chaabani, F., Proust D., Vieillard P., (2014). Mineralogical and
 574 geochemical signatures of clays associated with rhyodacites in the Nefza area
 575 (northern Tunisia). *Journal of African Earth Sciences* Volume 100, December 2014,
 576 Pages 267-277. <https://doi.org/10.1016/j.jafrearsci.2014.06.024>

577 Talbi F., Melki F., Ben Ismail-Lattrache K., Alouani R., Tlig S., (2008). Le Numidien
 578 de la Tunisie septentrionale: données stratigraphiques et interprétation
 579 géodynamique. *Estudios Geol.*, Vol. 64, n.º 1, 31-44, enero-junio. ISSN: 0367-0449.

580 Talbi, F., (1998). Petrologie, géochimie, études des phases fluides et gîtologie liées au
 581 magmatisme néogène de la Tunisie septentrionale. *Thèse de doctorat. Université*
 582 *Tunis II.* 368 pp.

583 Torres-Ruiz J., López-Galindo A., González M., Delgado A., (1994). Geochemistry of
 584 Spanish sepiolite–palygorskite deposits: genetic considerations based on trace
 585 elements and isotopes. *Chemical Geology*, 112, 221-245.
 586 [https://doi.org/10.1016/0009-2541\(94\)90026-4](https://doi.org/10.1016/0009-2541(94)90026-4)

- Trindade, M.J., Dias, M.I., Coroado, J., Rocha, F., (2009). Mineralogical transformations of calcareous rich clays with firing: a comparative study between calcite and dolomite rich clays from Algarve, Portugal. *Appl. Clay Sci.* 42, 345–355. <http://doi.org/10.1016/j.clay.2008.02.008>.
- Wezel, F. C., (1970). Numidian Flysch: an Oligocene-Early Miocene continental rize deposit of the African platform. *Nature* 228, 275-276.
- Wildi, W., (1983). La chaîne tello-rifaine (Algérie, Maroc, Tunisie): structure, stratigraphie et évolution du Trias au Miocène. *Rev. Géol. Dyn. Géogr. Phys.*, 24: 201-297.
- Yaich C., Hooyberghs H.J.F., Durllet C., Renard M., (2000). Corrélation stratigraphique entre les unités oligo-miocènes de Tunisie centrale et le Numidien. *C.R. Acad. Sci. Paris*, 331, 499-506. [https://doi.org/10.1016/S1251-8050\(00\)01443-9](https://doi.org/10.1016/S1251-8050(00)01443-9)
- Zouaoui H., & Bouaziz J. (2017). Physical and mechanical properties improvement of a porous clay ceramic. *Applied Clay Science*, 150, 131–137. doi:10.1016/j.clay.2017.09.002

Table Captions

Table1. Mineralogical (%) and chemical (wt.%) compositions of the studied samples.

Table 2. Ceramic tiles formulations.

Tables 3. Technological parameters of obtained ceramic products.

Figure Captions

Fig.1. Parts of geological map of Nefza (1) and Oued Sejnane (2) on scale 1/50.000 (Western southern area) showing the localization of the studied sections of Sidi Bader and Om Tebal.

Fig.2. Lithological sections of (1) Sidi Bader in the Tabarka area and Om Tebal in Sejnane area (2) (Felhi et al.. 2008; modified).

Fig. 3. Representation of the studied samples. using the Holtz & Kovacs (1981) diagram.

Fig. 4. Particle size distribution of the four clayey samples and the sand used in the mixture.

Fig. 5. Bigot curves of some clayey samples.

Fig. 6. DTA-TG curves of samples O1 and S8.

Fig. 7. Dilatometric curves of the studied samples grouped by site.

Fig. 8. Variation of the firing shrinkage of the ceramics tiles and the water absorption.

Fig.9: XRD patterns of S8 clay and the ceramic tiles resulting from mixture MS8 fired at various temperatures (1000°C. 1050°C. 1100°C and 1150°C); Qz: quartz; He: hematite; Mu: mullite; Di: diopside; Kao: kaolinite; Ill: illite

Fig. 10: XRD patterns of O1 clay and the ceramic tiles resulting from mixture MO1 fired at various temperatures (1000°C. 1050°C. 1100°C and 1150°C); Al: albite; Qz: quartz; He: hematite; Mu: mullite; Di: diopside; Kao: kaolinite; Ill: illite.

Fig. 11: Scanning electron micrographs of tiles from mixtures MS8 and MO1.

633 Table1. Mineralogical (%) and chemical (wt.%) compositions of the studied samples.

Mineralogy (%)											
	I-S	Illite	Kaolinite	Quartz	Calcite	Siderite					
O1	7	2	44	36	0	11					
O4	0	23	52	25	0	0					
S8	0	29	37	34	0	0					
S9	0	11	52	37	0	0					
RGS	0	11	45	30	14	0					
Stat. dev.	3(%)	3(%)	3(%)	3(%)	3(%)	3(%)					
Chemical analysis (wt.%)											
	SiO ₂	Al ₂ O ₃	Fe ₂ O ₃	MnO	MgO	CaO	Na ₂ O	K ₂ O	TiO ₂	P ₂ O ₅	L.O.I
O1	59.42	17.94	7.58	0.01	1.65	0.53	1.01	0.16	0.78	0.13	9.77
O4	57.31	19.75	6.99	0.02	1.62	0.49	0.03	2.01	0.66	0.12	8.77
S8	57.73	26.33	1.82	0.002	0.56	0.27	0.09	2.2	1.32	0.46	10.52
S9	60.58	25.08	1.96	0.01	0.64	0.17	0.04	2.15	1.42	0.32	10.78
RGS	46.3	20.7	6.69	0.01	0.86	8.05	0.2	1.5	0.9	0.2	14.35
Stat. dev.	0.1	0.048	0.006	0.001	0.0072	0.012	0.017	0.017	0.0051	0.0074	

Stat. dev. :Standard deviation

659 Table 2. Ceramic tiles formulations.

	Clays (wt. %)					Sand (wt. %)	Feldspar (wt. %)
	S8	S9	O1	O4	RGS		
S8	100	-	-	-	0	0	0
S9	-	100	-	-	0	0	0
O1	-	-	100	-	0	0	0
O4	-	-	-	100	0	0	0
MS8	60	-	-	-	20	15	5
MS9	-	60	-	-	20	15	5
MO1	-	-	70		20	5	5
MO4	-	-	-	70	20	5	5

660

661

662

663

664

665

666

667

668

669

670

671

672

673

674

675

676

677

678 Table 3. Technological parameters of obtained ceramic products.

Raw	Firing shrinkage(%)				Water absorption(%)				Bending strength (N/mm ²)			
	S8	S9	O1	O4	S8	S9	O1	O4	S8	S9	O1	O4
Drying shr.	1.11	0.21	1.55	1.47	-	-	-	-	-	-	-	-
1000°C	0.93	0.23	0.9	0.53	19.42	13.87	13.07	15.41	0.95	0.65	2.24	0.97
1050°C	1.32	0.3	1.74	1.49	15.72	13.74	14.12	14.78	1.12	0.87	2.58	1.59
1100°C	1.54	0.78	3.29	1.55	14.82	12.17	11.2	14.63	1.29	1.31	4.06	3.07
1150°C	1.82	0.64	4.42	5.73	13.76	13.27	9.13	8.38	1.46	1.25	2.95	5.31
Stat. dev.	0.02	0.02	0.02	0.02	1	1	1	1	0.02	0.02	0.02	0.02
Mixtures	MS8	MS9	MO1	MO4	MS8	MS9	MO1	MO4	MS8	MS9	MO1	MO4
Drying shr.	0.02	0.19	0.42	0.54	-	-	-	-	-	-	-	-
1000°C	0.44	0.30	1.15	1.10	14.47	12.93	13.79	13.62	13.17	13.16	14.63	14.66
1050°C	0.74	0.53	1.77	1.64	14.47	12.53	12.43	12.33	13.28	13.36	15.63	15.56
1100°C	1.21	0.55	1.98	1.80	14.10	12.13	11.86	12.68	13.69	13.5	15.07	15.22
1150°C	2.00	1.02	2.14	2.54	11.95	11.48	10.98	11.47	15.31	13.66	15.95	15.67
Stat. dev.	0.02	0.02	0.02	0.02	1	1	1	1	0.02	0.02	0.02	0.02

679 Drying shr : Drying Shrinkage; Stat. dev. :Standard deviation

680

681

682

683

684

685

686

687

688

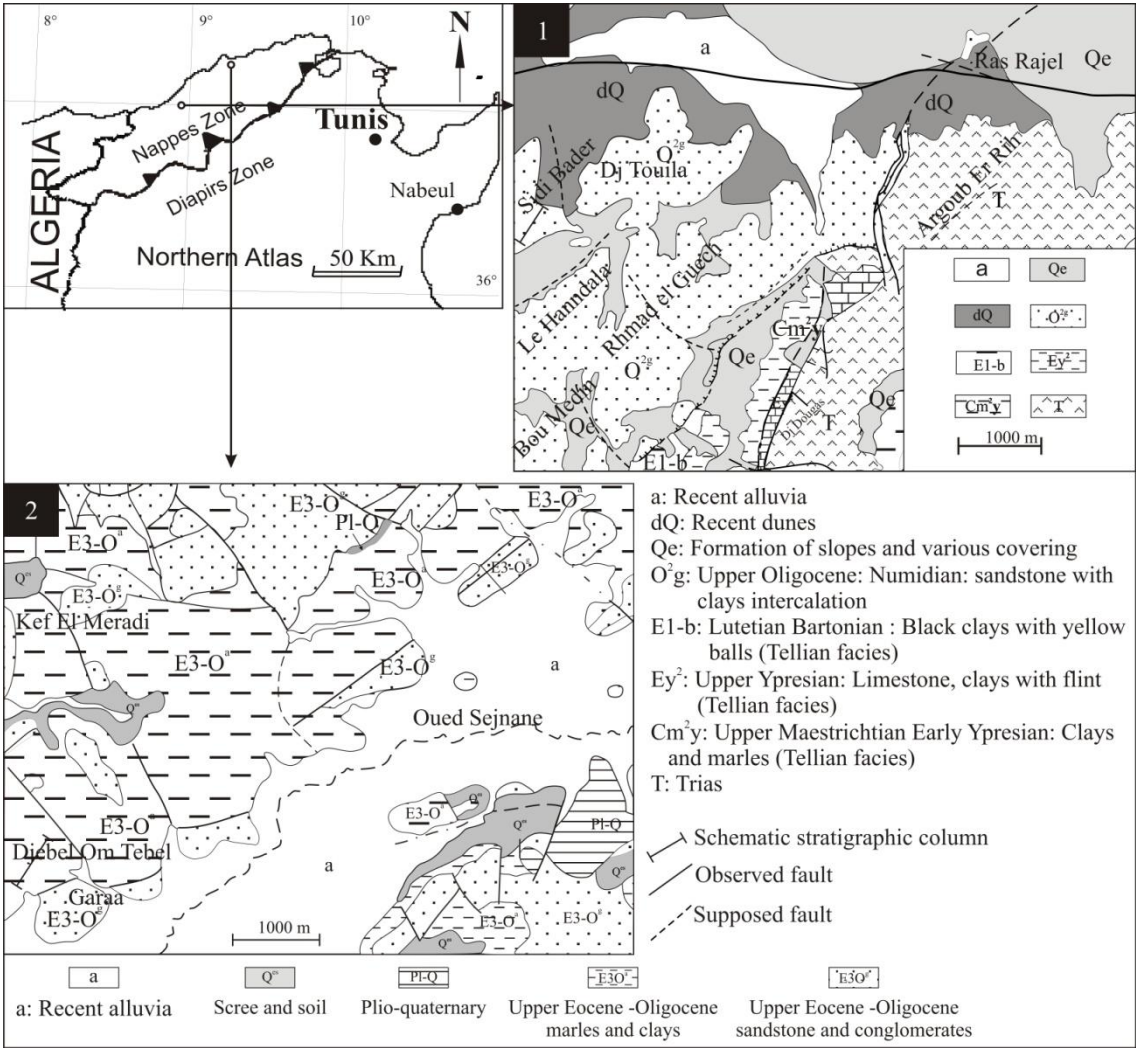
689

690

691

692

693 Fig. 1



694
695 Fig.1. Parts of geological map of Nefza (1) and Oued Sejnane (2) on scale 1/50.000
696 (Western southern area) showing the localization of the studied sections of Sidi Bader
697 and Om Tebal.

Fig. 2

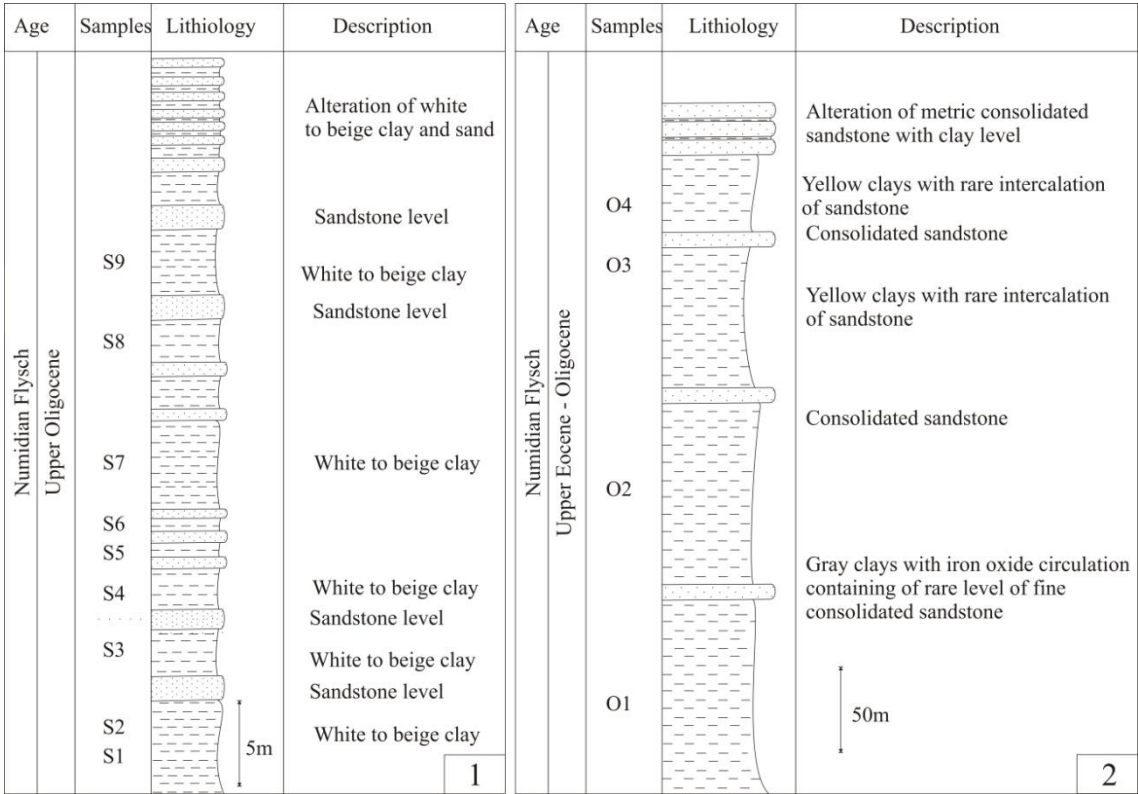


Fig.2. Lithological sections of (1) Sidi Bader in the Tabarka area and Om Tebal in Sejnane area (2) (Felhi et al.. 2008; modified).

Fig. 3

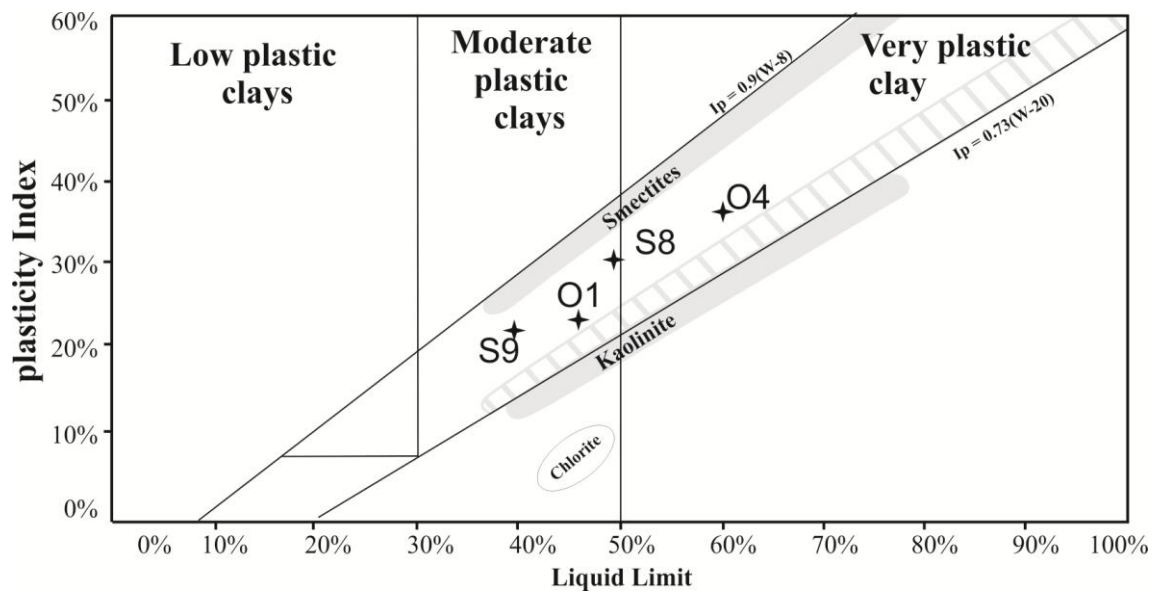


Fig. 3. Representation of the studied samples. using the Holtz & Kovacs (1981) diagram.

Fig. 4

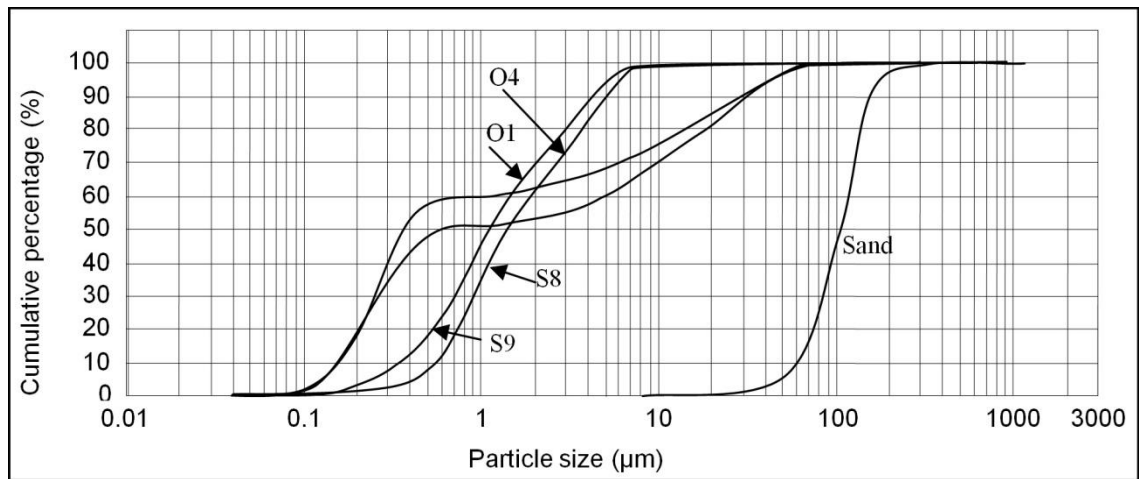


Fig. 4. Particle size distribution of the four clayey samples and the sand used in the mixture.

Fig. 5

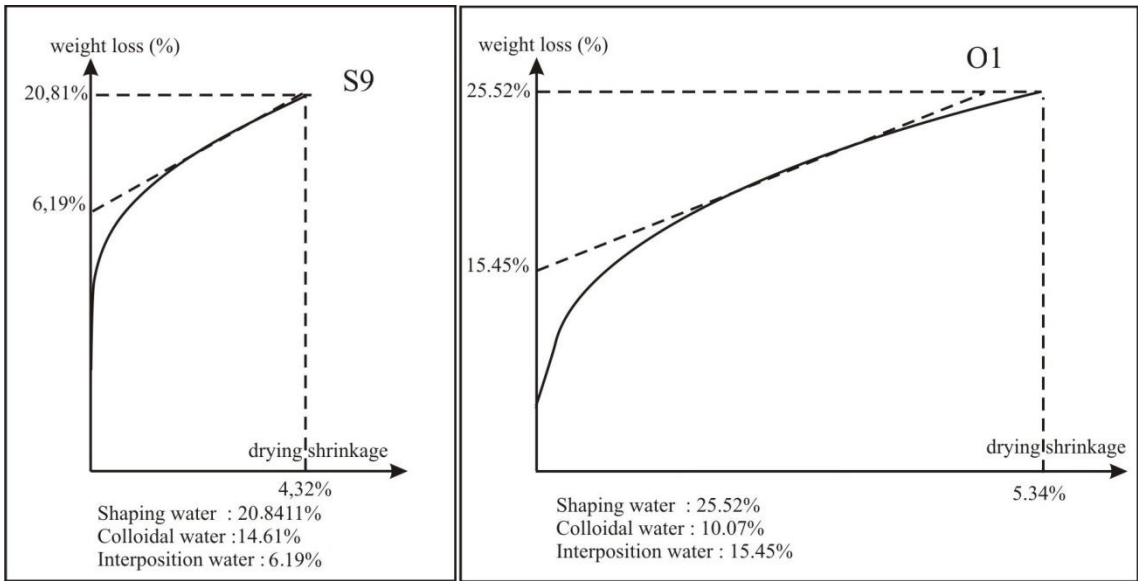


Fig. 5. Bigot curves of some clayey samples.

Fig. 6

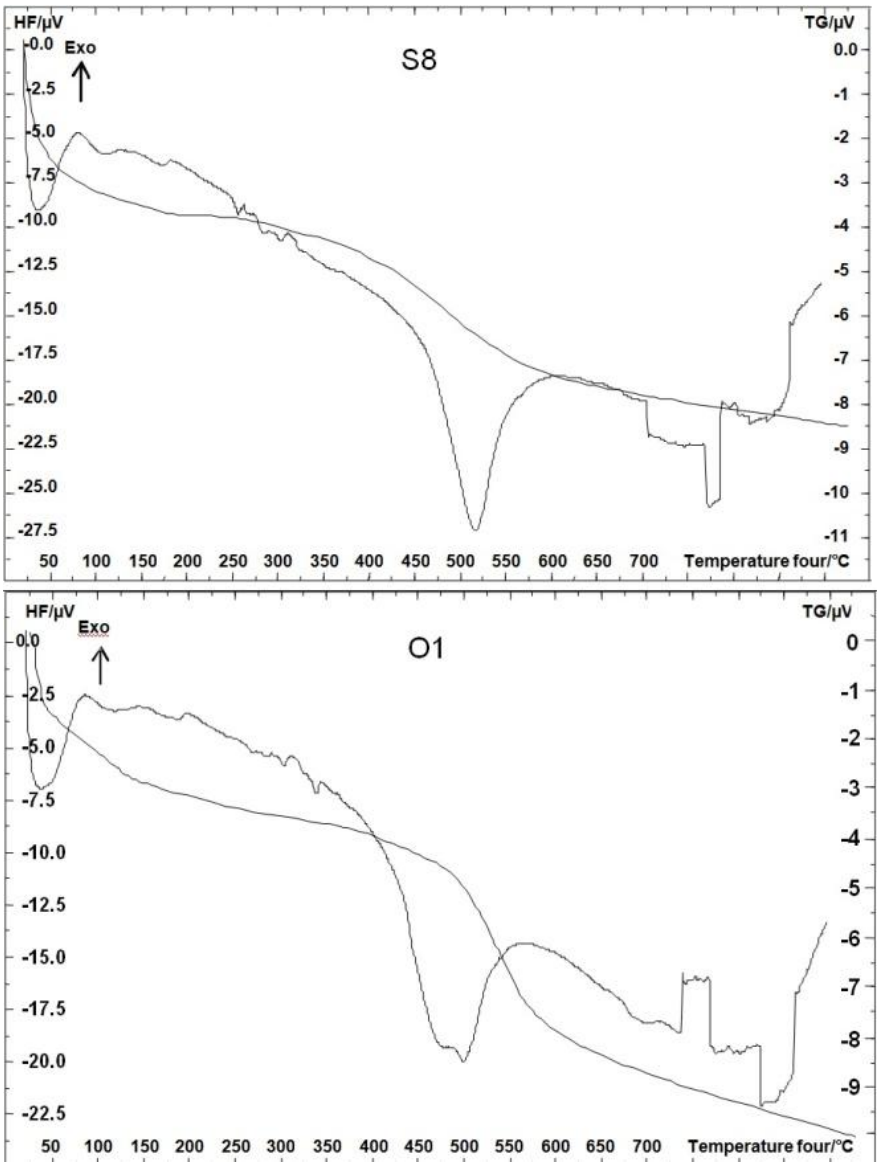


Fig. 6. DTA-TG curves of samples O1 and S8.

Fig. 7

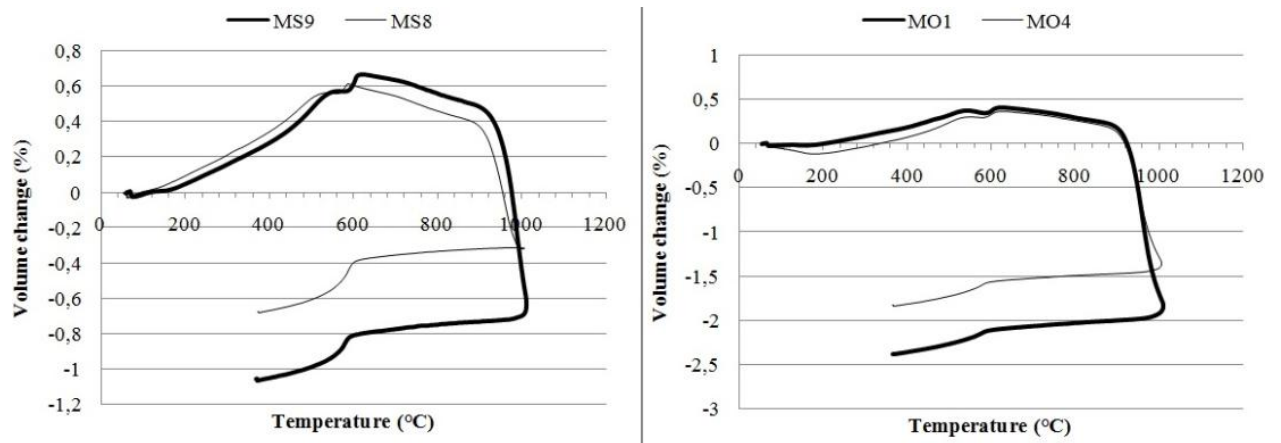
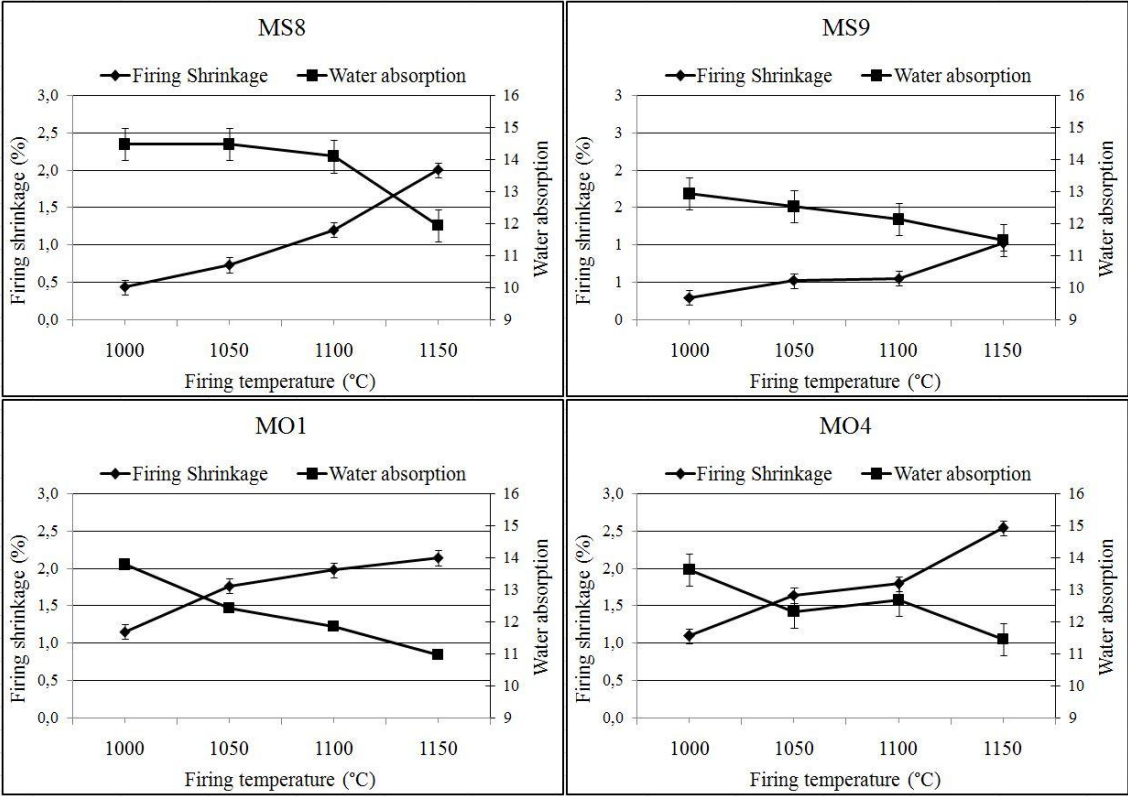


Fig. 7. Dilatometric curves of the studied samples grouped by site.

801 Fig. 8



802

803 Fig. 8. Variation of the firing shrinkage of the ceramics tiles and the water absorption.

804

805

806

807

808

809

810

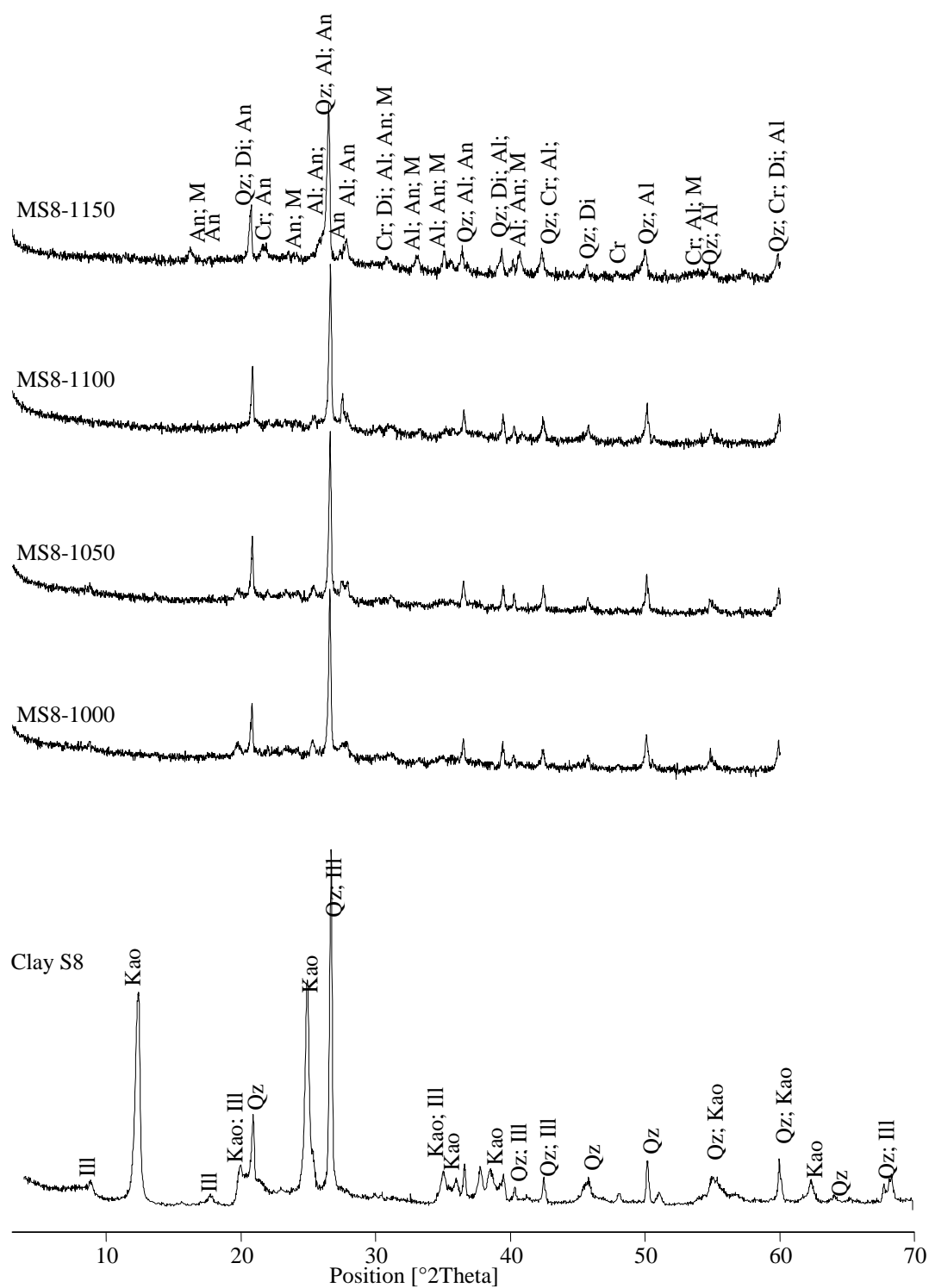
811

812

813

814

815 Fig. 9



816

817 Fig.9: XRD patterns of S8 clay and the ceramic tiles resulting from mixture MS8 fired

818 at various temperatures (1000°C. 1050°C. 1100°C and 1150°C); Qz: quartz; He:

819 hematite; Mu: mullite; Di: diopside; Kao: kaolinite; Ill: illite

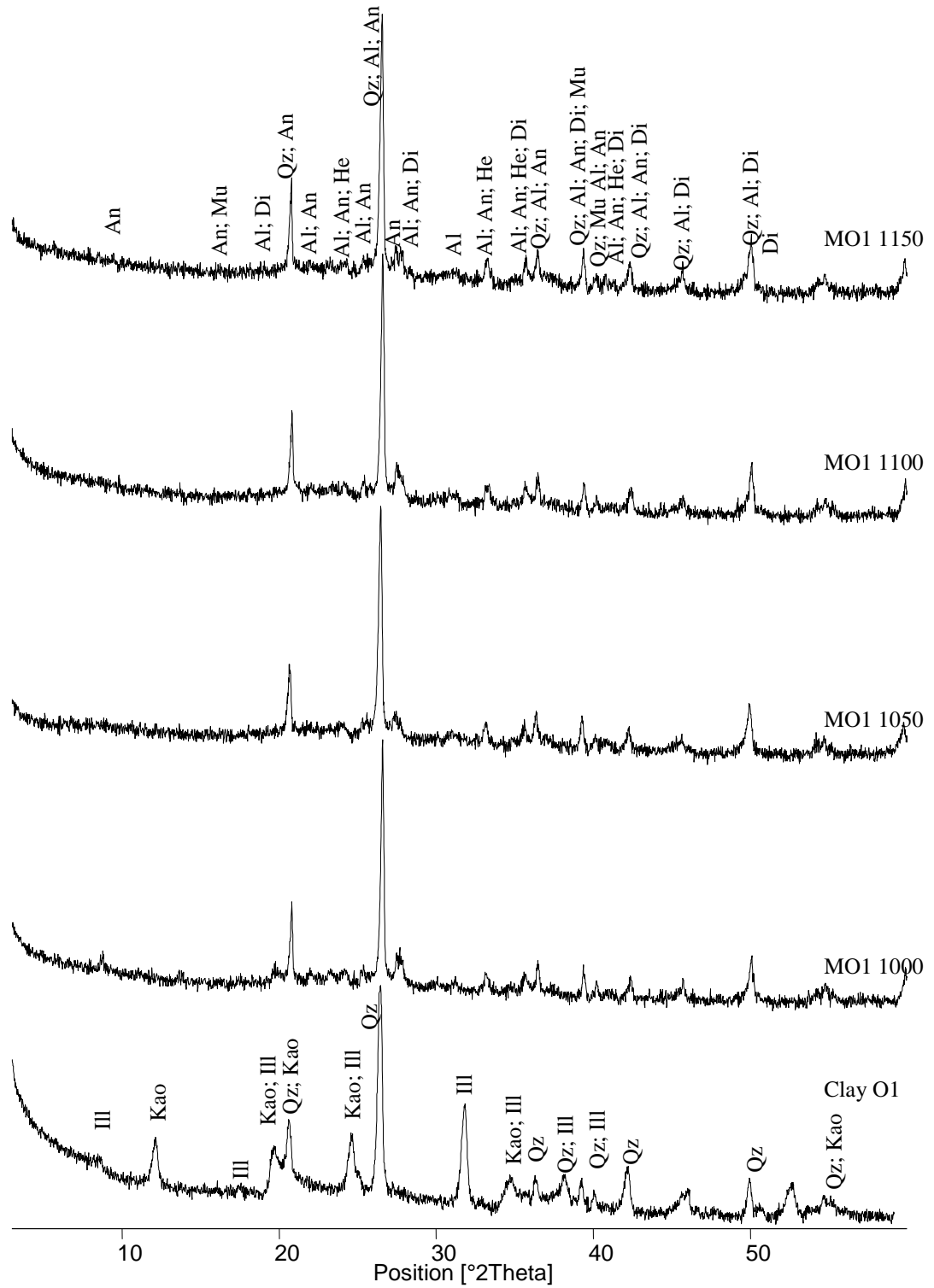
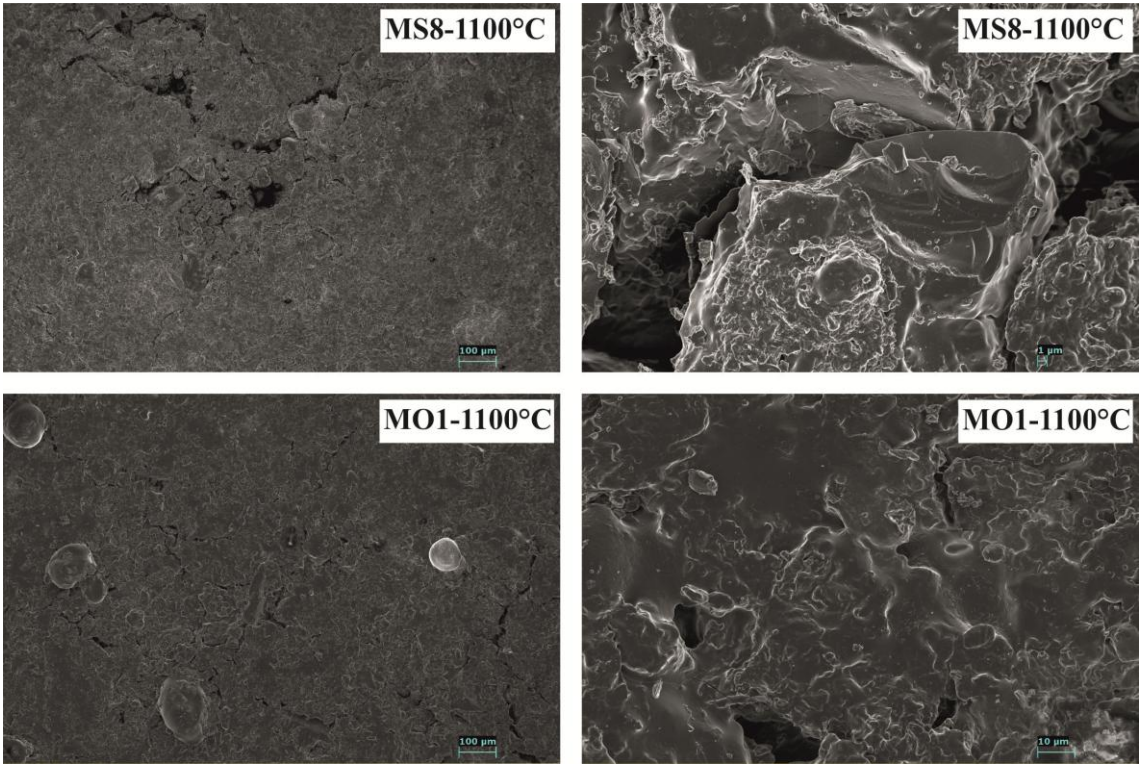


Fig. 10: XRD patterns of O1 clay and the ceramic tiles resulting from mixture MO1 fired at various temperatures (1000°C. 1050°C. 1100°C and 1150°C); Al: albite; Qz: quartz; He: hematite; Mu: mullite; Di: diopside; Kao: kaolinite; Ill: illite.

825 Fig. 11



826

827 Fig. 11: Scanning electron micrographs of tiles from mixtures MS8 and MO1.

828

829

Title page:

Numidian clay deposits as raw material for ceramics tile manufacturing

Declaration of Interest Statement

I declare that this article is original work. The co-authors have confirmed the existence of their names in this paper

☒ We confirm that the manuscript has been read and approved by all named authors.

☒ We confirm that the order of authors listed in the manuscript has been approved by all named authors.